# Testing the capabilities of the Mars Organic Molecule Analyser (MOMA) chromatographic columns for the separation of organic compounds on Mars

Melissa Guzman, Cyril Szopa, Caroline Freissinet, Arnaud Buch, Fabien
Stalport, Desmond Kaplan, François Raulin

# Testing the capabilities of the Mars Organic Molecule Analyser (MOMA) chromatographic columns for the separation of organic compounds on Mars

Melissa Guzman [a,*], Cyril Szopa [a,b], Caroline Freissinet [a], Arnaud Buch [c], Fabien Stalport [d], Desmond Kaplan [e], François Raulin [d]

[a] LATMOS/IPSL, UVSQ Université Paris-Saclay, Sorbonne Université, CNRS, Guyancourt, France
[b] Institut Universitaire de France, Paris, France
[c] Laboratoire de Génie des Procédés et Matériaux, Ecole Centrale Supelec, Gif-sur-Yvette, France
[d] Laboratoire Interuniversitaire des Systèmes Atmosphériques, UMR CNRS 7583, Université Paris Est, Créteil Université de Paris, Institut Pierre Simon Laplace, France
[e] KapScience LLC, Tewksbury, MA, USA

## ABSTRACT

Mars is our planetary neighbor and is now known to host trace levels of organic matter at its surface. However, little is known of the organic molecular composition or the survival potential for organic biosignatures, such as the enantiomeric excess of amino acids or the carbon chain patterns of lipid hydrocarbons, as a function of depth below the martian surface. The Mars Organic Molecule Analyser (MOMA) is an instrument onboard the Rosalind Franklin rover that is scheduled to be launched to Mars in 2022 as part of the ExoMars mission. This experiment includes a gas chromatograph instrument dedicated to the *in situ* analysis of organic molecules and their enantiomers present in martian samples collected by the rover at the surface down to 2 m depth. In order to evaluate the performance of the integrated chromatographic system which was selected for the flight model, experiments were carried out with a laboratory setup that reproduced the flight configuration and mimicked the *in situ* operating conditions. We show that the column instrument package can separate and detect a wide range of organic and inorganic volatile compounds, from noble gases to hydrocarbon chains with up to 29 carbon atoms ($C_{29}$). We study the enantiomeric resolution of selected chiral chemical standards and compare our laboratory results to: i. tests performed with the same instrumental setup but using a natural sample spiked with amino acids in order to evaluate the influence of a mineral phase on the analysis, and ii. tests run on a MOMA engineering test unit (ETU) which is representative of the flight model. In each case, tests on the more complex sample and the more flight-like instrument allow a comparison with laboratory results, in order to confirm that laboratory data are reliable for supporting peak identification within flight data. The obtained results demonstrate the ability of the gas chromatographic subsystem to identify a wide range of organic and inorganic volatile compounds, including biomolecular signatures, within the constrained space operating conditions of MOMA. The results form a retention time and mass spectral database for MOMA which will be critical for analysis of the eventual flight data.

## 1. Introduction

Gas chromatography coupled to mass spectrometry (GC-MS) was first used for *in situ* Mars exploration by the twin Viking landers, which arrived on Mars in 1976 with the aim of searching for signs of life in the near surface environment. In support of the three Viking biology experiments, the Viking landers conducted an organic inventory of the martian regolith, since primitive life on Earth is understood to have originated from the processing of organic molecules by liquid water (Brack, 2010). The Viking GC-MS experiment did not detect organic molecules, with the exception of chloromethane (detected by Viking Lander 1 at levels of 15 parts per billion by mass) and dichloromethane (detected by Viking Lander 2 at levels of 2–40 parts per billion by mass). These signals were at first attributed to cleaning agents used on the spacecraft before launch (Biemann et al., 1977). Despite the open question of whether or not the

Viking landers detected organics native to Mars (Guzman et al., 2018; Navarro-González et al., 2010), their results represent a paradigm shift within Mars astrobiology exploration. The possibility of widespread microbial life at the martian surface was replaced with an understanding that, given such low detection limits for organic compounds determined at the time of the Viking results, it is difficult to maintain that living organisms based on the terrestrial carbon-hydrogen-nitrogen-oxygen chemistry are widely distributed at the surface of Mars (Biemann et al., 1977; Pavlov et al., 2012).

Additionally, the Viking GC-MS results required a mechanism for the destruction of organic molecules at Mars. It was understood then and has now been estimated that significant amounts of carbon material are delivered to the martian surface each year from at least the interplanetary medium (Flynn, 1996). Since the Viking result, radiation has been studied as a degradation and alteration mechanism for organic matter in

* Corresponding author.
  *E-mail address:* melissa.guzman@latmos.ipsl.fr (M. Guzman).

the context of Mars, *e.g.*, the influence of the ultraviolet radiation environment on organic matter at the martian surface (Stalport et al., 2019). The Viking result also suggested a powerful oxidant capable of converting all organic molecules in the martian regolith to carbon dioxide rapidly relative to the rate at which they arrive from exogenous sources (Benner et al., 2000). In fact, there are now multiple oxidants assumed to be present at the martian surface or which have been detected already on Mars (Lasne et al., 2016). The 2008 Phoenix mission confirmed the presence of oxychlorine phases in the form of perchlorates at the northern pole of Mars (Hecht et al., 2009). Perchlorates have also been studied at Gale Crater by the GC-MS instrument within the Curiosity rover's Sample Analysis at Mars (SAM) instrument suite (Leshin et al., 2013; Sutter et al., 2017). The unexpected discovery of perchlorates by Phoenix resulted in another paradigm shift in which the community began to question if pyrolysis-GC-MS could enable the detection of trace levels of organics (Navarro-González et al., 2010). Curiosity's SAM instrument, in addition to significantly advancing our understanding of martian habitability, has shown that a GC-MS instrument can detect organics in martian samples collected within the 5 cm drill capability of the Curiosity rover despite the challenges of perchlorates (Eigenbrode et al., 2018; Freissinet et al., 2015; Szopa et al., 2020).

The Mars Organic Molecule Analyser (MOMA) experiment is scheduled to travel to Mars onboard the Rosalind Franklin rover of the joint ESA/Roscosmos ExoMars 2022 mission (Vago et al., 2017). MOMA is a miniaturized chemical laboratory specifically dedicated to analyzing the organic and inorganic content of samples collected by the rover at the martian surface and subsurface (Goesmann et al., 2017). Through these measurements, MOMA will contribute to characterizing the past and present habitability of Oxia Planum, the landing site selected for the rover, where features and minerals associated with flowing liquid water were observed from the Mars orbit (Quantin et al., 2016). MOMA will have the capability to detect non-statistical distributions of molecules, or molecular patterns of astrobiological interest, with the Laser Desorption/Ionization Mass Spectrometry (LDMS) mode. Laboratory experiments have shown the LDMS mode to be less sensitive to the presence of oxidizing reagents such as perchlorates (Li et al., 2015). MOMA will also have the capability to analyze drilled samples from up to 2 m in depth. These samples may be protected from the oxidation processes discussed

earlier and from solar and galactic radiation over geologic timescales (Pavlov et al., 2012). Therefore, they may contain more abundant and pristine organic materials.

MOMA includes a gas chromatographic (GC) package, developed from the experience acquired by our team from the SAM instrument, and an ion trap mass spectrometer (ITMS) (Brinckerhoff et al., 2013). The GC-MS will separate volatile and semi-volatile compounds within a sample after heating or chemical treatment and provide a spectral signature of each compound. This combination allows the strict identification of organic molecules. In order to achieve the separation of a wide range of volatile compounds potentially released from the sample, the GC is composed of four different and complementary analytical channels (Table 2), all including a capillary column dedicated to a specific range of chemical species. As on the Rosetta mission's Cometary Sampling and Composition (COSAC) experiment, MOMA will carry a chiral gas chromatographic column with the capability to separate molecular enantiomers of chiral compounds from various chemical families; in some cases, after the compounds are derivatized with the appropriate derivatization reagent (Freissinet et al., 2010; Meierhenrich et al., 2013; Myrgorodska et al., 2016). The use of a chiral column enables the extraterrestrial

**Table 2**

List of GC capillary columns selected for MOMA GC and their main characteristics.

| Name (Supplier) | Stationary Phase | Dimensions L/ID/$d_f$ (m/mm/μm) | Compounds targeted |
|---|---|---|---|
| MXT Q BOND (Restek) | Divinylbenzene | 20/0.25/8 | Inorganic volatile molecules $C_1$–$C_5$ organic molecules |
| MXT CLP (Restek) | Not available from the supplier | 20/0.25/0.25 | $C_4$–$C_{25}$ organic molecules |
| MXT 5 (Restek) | 95% dimethylsiloxane 5% diphenylsiloxane | 20/0.25/0.25 | $C_4$–$C_{25}$ organic molecules |
| CP Chirasil Dex CB (Agilent) | Enantioselective, β-cyclodextrin bonded to dimethylpolysiloxane | 20/0.25/0.25 | Organic enantiomers |

**Table 1**

List of chemical standards tested on GC columns. The derivatization reagents cited in the last column were used for each of the GC columns listed in the corresponding first column. *Alcohols were not derivatized for studying the MXT Q BOND column since the underivatized alcohols had already sufficiently high retention times within the nominal 35-min run time.

| Column | Family | Chemical Standard | Solvent and Concentration | Derivatization Agent |
|---|---|---|---|---|
| CP Chirasil Dex | Alcohols | $C_2$ to $C_9$ linear alcohols | $10^{-4}$ vol% in methanol (for non-derivatized alcohols) | Tests were conducted with no derivatization and with derivatization (DMF-DMA, MTBSTFA/DMF) |
| MXT-5 MXT-CLP | Alkanes | $C_7$ to $C_{40}$ linear and ramified alkanes | 1 g·L$^{-1}$ in hexane | N/A |
| | Carboxylic acids | Oxalic acid Benzoic acid Hexanoic acid Octanoic acid Nonanoic acid Decanoic acid Dodecanoic acid Mellitic acid | $10^{-2}$ mol·L$^{-1}$ in demineralized water | Carboxylic acids were derivatized with DMF-DMA and MTBSTFA/DMF |
| | Amino acids | Glycine DL-alanine DL-valine DL-glutamic acid DL-serine DL-leucine | $10^{-2}$ mol·L$^{-1}$ in demineralized water | Amino acids were derivatized with DMF-DMA and MTBSTFA/DMF |
| CP Chirasil Dex | Alkanes | 3-methylhexane, 3-methylheptane | $10^{-3}$ vol% in cyclohexane | N/A |
| MXT Q BOND | Alcohols | $C_2$ to $C_5$ linear alcohols | $10^{-4}$ vol% methanol | N/A* |
| | Noble Gases | Neon, Argon, Krypton, Xenon | 15 mol.%, 5 mol.%, 3 mol.%, 2 mol.% in helium | N/A |
| | Hydrocarbons | Ethane, Ethylene, Butane, Pentane | 0.0095675% (butane), 0.0099951% (pentane) in helium; concentration for ethane and ethylene not available | N/A |

determination and quantification of the enantiomeric excess of chiral molecules. The quantification of enantiomeric excess could reveal information about whether martian organic enantiomers are in a racemic ratio, if they express an enantiomeric bias, or even homochirality, a molecular quality considered to be a signature of terrestrial biology.

Additionally, some of the compounds of astrobiological interest for MOMA, and specifically those biomolecules displaying the property of homochirality in terrestrial life (*e.g.*, amino acids), contain labile hydrogen atoms in polar functional group (*e.g.*, –OH, –COOH, –NH, –SH, or -PH). These kinds of compounds tend to self-react or to be strongly adsorbed by the GC column stationary phase, which prevent their analysis by GC-MS. To overcome this analytical problem, a derivatization reagent can be utilized to produce controlled reactions which protect the reaction group against unwanted reactions and thermal destabilization (Knapp, 1979). MOMA carries three different chemical reagents, *N, N*-Dimethylformamide dimethyl acetal (DMF-DMA) and *N*-methyl--*N-tert*-butyl-dimethylsilyltrifluoroacetamide (MTBSTFA) for derivatization and tetramethylammonium hydroxide (TMAH) for thermochemolysis, each one with the capability to reveal specific properties of organic molecules. DMF-DMA is the only reagent selected which enables the detection of molecular enantiomers and has so far never been utilized in the analysis of martian samples. The MOMA gas chromatographic package is heavily aided by these wet chemistry capabilities in order to meet its objectives, both to enable the detection of molecules with labile polar functional groups and, in the case of DMF-DMA, to enable the detection of molecular enantiomers.

The flight model (FM) of MOMA is now finalized and integrated in the rover, and the range of operating conditions of the instrument under the Mars surface environmental conditions has been constrained (e.g., carrier gas flow rates, transfer line temperatures). Expected GC-MS operating conditions for Mars are shown in Table 3. The aim of this paper is to present the final chromatographic column package selected for MOMA, the analytical procedures that will be used on Mars, a retention time and mass spectral library to support the analyses of eventual Mars flight data, and a demonstration of the analytical performance of a laboratory system that simulates the flight experiment and the *in situ* operating conditions. We give special attention to the enantiomeric separation capabilities

**Table 3**

Technical parameters of the GC-MS analysis between the FM and in the laboratory. We include the derivatization-GC-MS parameters here, since pyrolysis-GC-MS has not been studied in this work. However, it is expected that the maximum temperature of the pyrolysis ovens will be 800 to 850 °C (Goesmann et al., 2017).

| Experimental component | Parameter | Flight Model | Laboratory GC-MS |
|---|---|---|---|
| Ovens, transfer lines, and trap | $T_{max}$ derivatization oven (°C) | 600 | Optimized derivatization temperatures for standards (75 °C for MTBSTFA; 140 °C for DMF-DMA) |
| | $T_{max}$ transfer lines (°C) | ≥135 | 250 (GC-MS transfer line) |
| | $T_{max}$ trap (°C) | 300 | No trap |
| | Trap flow mode | Supports flow inversion | No flow inversion |
| GC | $T_i$ (°C) | ≥30 | 35–45 |
| | Ramp rate (°C·min$^{-1}$) | 1–15 | 3–10 |
| | $T_f$ (°C) | 220 °C (MXT 5, MXT CLP) 180 °C (Chirasil Dex) 200 °C (Q BOND) | 220 °C (MXT 5, MXT CLP) 180 °C (Chirasil Dex) 200 °C (Q BOND) |
| | He flow rate (mL·min$^{-1}$) | 0.8 to 1.4 mL·min$^{-1}$ (adjustability); 1.2 mL·min$^{-1}$ (nominal) | 0.2 to 2 mL·min$^{-1}$ |
| MS | Mass range (*m/z*) | 50–500 | 10–500 |

which have not been performed on Mars before. A set of chemical compounds of interest for Mars near-surface science and astrobiology was selected and analyzed across each of the four columns. We show that the column instrument package can separate and detect a wide range of organic and inorganic volatile compounds, from noble gases to hydrocarbon chains with up to 29 carbon atoms ($C_{29}$). Next, a study of selected chiral chemical standards demonstrates the analytical performance of the chiral column based on enantiomeric resolution of these molecules. The results of the laboratory chiral studies were compared to tests performed with the same laboratory setup but using a natural sample, which included a mineral phase, spiked with amino acids, in order to test a more realistic case. The laboratory chiral studies were also compared to tests run on a MOMA engineering test unit (ETU) to show the relevance and utility of column testing performed in the laboratory for interpretation and data treatment of MOMA flight data. Because any planetary instrument with the capability to enable biosignature detection is unlikely to demonstrate a single indisputable positive result, it is critical to produce a group of complimentary observations to be assessed together for interpretation. We demonstrate the capability of the chromatographic column package to detect multiple parameters indicative of terrestrial biology.

## 2. Materials and methods

### 2.1. Samples

#### 2.1.1. Selection of standards

Among the chemical families of organic molecules that can be deposited on Mars via exogenous sources and/or synthesized on Mars endogenously, the number of organic species that could be tested experimentally is too large to lead a systematic study in a reasonable amount of time. Therefore, the following specific chemical families, and specific molecules within those families, have been selected for our study of the MOMA GC columns and are summarized in Table 1. The compounds are appropriate for the design requirements outlined for the main classes of chemical species to be separated by the MOMA GC columns (Goesmann et al., 2017).

The organic compounds selected for this study were targeted according to several criteria:

- Potential to elute across a range of retention times from the GC columns, *e.g.* linear and ramified alkanes with a molecular mass range from 100.21 g·mol$^{-1}$ (heptane) to 563.08 g·mol$^{-1}$ (tetracontane).
- Representatives of several key families of molecules, thus several physio-chemical characteristics, *e.g.* alkanes without a labile polar functional group versus alcohols with an –OH chemical function.
- Potential presence in the samples that can be collected at Mars's surface and sub-surface, *i.e.* the molecules selected are among the most abundant within known exogenous sources or correspond to evolution products of organic molecules under Martian environmental conditions, *e.g.* carboxylic acids as products of oxidation (Benner et al., 2000) and potential precursors to previously detected chlorinated hydrocarbons (Miller et al., 2016).
- Organic molecules of interest for astrobiology, *e.g.* chiral amino acids.

Amino and carboxylic acids are particularly interesting for testing on the MOMA gas chromatographic package, since they are of particular interest for astrobiology (Davila and McKay, 2014), require derivatization for optimal detection by GC-MS (Freissinet et al., 2010), and have been detected in meteorites and comets (Altwegg et al., 2016; Glavin et al., 1999, 2004; Sephton, 2012). Among our selected amino acids, only glycine does not possess the property of chirality. Glycine ($C_2H_5NO_2$) and alanine ($C_3H_7NO_2$) have both been detected in micrometeorites and carbonaceous chondrites (Ehrenfreund et al., 2001; Maurette, 1998; Pizzarello et al., 2006; Sephton, 2005; Sephton and Botta, 2008), and, in the case of glycine, in comet material (Altwegg et al., 2016; Elsila et al., 2009). In addition to the potential for amino acids to be brought to the

surface of Mars by exogenous sources, they can be synthesized by various endogenous and abiotic processes, such as via hydrothermal vents (Hennet et al., 1992; Marshall, 1994), atmospheric processes (Cleaves et al., 2008), and under the influence of irradiation (Kobayashi et al., 1995).

The selected amino acids include those heavily studied (glycine) and largely undiscussed (glutamic acid) in relation to martian environmental conditions. The potential evolution of glycine under martian environmental conditions has been a topic of numerous experimental studies (Oró and Holzer, 1979; Poch et al., 2014; Stoker and Bullock, 1997; ten Kate et al., 2006). While laboratory studies show that alanine is unstable in the martian oxidation surface environment (Benner et al., 2000) and under martian surface UV radiation (ten Kate et al., 2006), studies have shown it would be preserved in minerals such as magnesium sulfates (François et al., 2016) and clays (Bowden and Parnell, 2007; Kennedy et al., 2002) and its potential subsurface stability may be elucidated by MOMA.

Of the carboxylic acids, oxalic acid is the most abundant dicarboxylic acid in several carbonaceous chondrites (Peltzer et al., 1984; Pizzarello and Garvie, 2014; Shimoyama and Shigematsu, 1994). Benzoic and mellitic acids have both been proposed as metastable and stable intermediate oxidation state molecules formed from polycyclic aromatic hydrocarbons (PAHs) potentially provided by exogenous sources (Benner et al., 2000). Mellitic acid has been studied under martian irradiation conditions (Poch et al., 2014; Stalport et al., 2009) and would be destroyed by nearly 63% after a few hours of irradiation in addition to undergoing dehydration leading to the formation of mellitic acid trianhydride (Archer, 2010; Stalport et al., 2019). In addition to aromatic and di-carboxylic acids, we tested several long chain carboxylic acids which, although terrestrial contamination cannot be ruled out, have been detected in carbonaceous chondrites with between 13 and 23 carbon atoms (Murchison) and with between 2 and 12 carbon atoms (Asuka-881458) (Deamer and Pashley, 1989; Naraoka et al., 1999).

### 2.1.2. Non-derivatized standards

For the laboratory experiments, the non-derivatized linear alcohols were diluted in methanol at $10^{-4}$ vol% in order to inject precise amounts of chemical standards and without risking saturation of the stationary phases or detector. For the same reason, the $C_7$ to $C_{40}$ linear alkanes were diluted in hexane at a 1 g·L$^{-1}$ mass concentration. The 3-methylhexane and 3-methylheptane were diluted in cyclohexane at $10^{-3}$ vol%. Liquid and solid compounds were supplied by Sigma-Aldrich, whereas gaseous components were supplied by Air Liquide, Linde and Messer. 0.5 μL of the liquid solutions were injected into the GC-MS using a 1 μL liquid syringe (SGE) and 1 mL of the gas mixtures were injected using a 5 mL gas syringe (SGE). Fig. 2 shows a run with no syringe injection performed directly
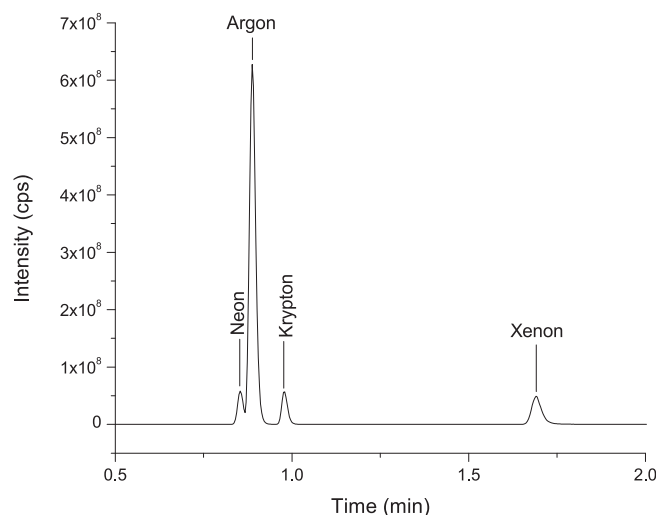


**Fig. 2.** Noble gases separated on the MXT Q BOND. The GC column was held at 35 °C for 7 min, then heated to 182 °C with a 3°C·min$^{-1}$ ramp. The Ar response is high compared to the other noble gases, considering the relative ratios of the gases, because Ar was mixed with some air ($N_2$ and $O_2$) that entered the syringe before injection.

after a run with a 1 mL syringe injection of the noble gas mixture due to saturation of the column with this high injection volume.

### 2.1.3. Derivatized standards

MTBSTFA is a silylation reagent that reacts with a wide range of functional groups by replacing labile hydrogen with a tert-butyl-dimethylsilyl group (Si(CH$_3$)$_2$C(CH$_3$)$_3$ or TBDMS), as shown in Fig. 5 (Mawhinney and Madson, 1982). This derivatization reagent was used for the first time in space exploration in the SAM experiment onboard the Mars Curiosity rover (Mahaffy et al., 2012). Despite its high reaction yield, disadvantages of using MTBSTFA include sizable background signals of reaction byproducts such as *tert*-butyldimethylsilanol (monosilylated water or MSW) and 1,3-bis(1,1-dimethylethyl)-1,1,3,3-tetramethyldisiloxane (bisilylated water or BSW). The second derivatization reagent utilized by MOMA, DMF-DMA, is a reagent that replaces a labile hydrogen atom by a methyl group or by a trimethylformamidine group on the amine part of the molecule (Freissinet et al., 2010; Meier-henrich et al., 2001). Although DMF-DMA has a lower reaction yield than MTBSTFA, it has the capability to enable separation of enantiomers when used with an enantioselective column (Freissinet et al., 2010). The use of TMAH enables the technique of thermochemolysis on MOMA, which
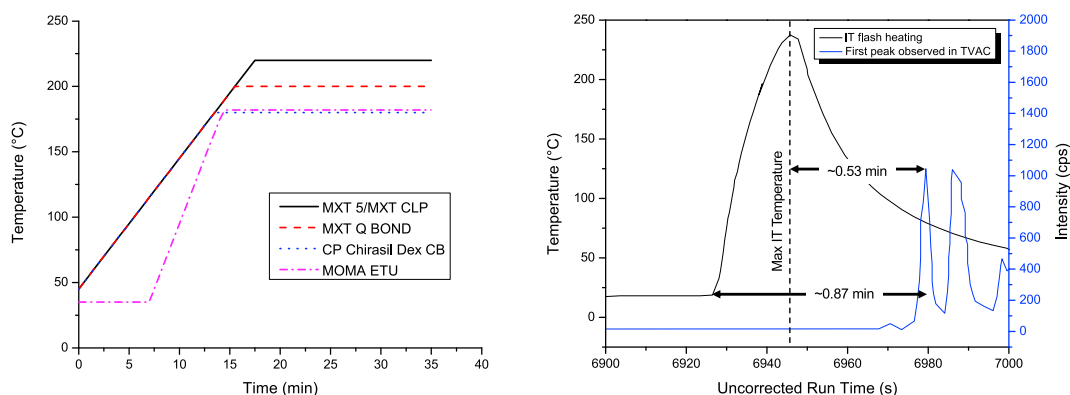


**Figure 1.** (Left) Comparison of main column temperature programs used for characterization of the MOMA GC columns in a laboratory setting. We show the nominal MOMA temperature curves used for the study of chemical standards on each of the four columns (MXT 5/CLP, MXT Q BOND, and CP Chirasil Dex CB), as well as the temperature program used for the study of enantiomeric resolution of chiral compounds on the MOMA chiral column, which was meant to mimic the ETU tests. (Right) The MOMA injection trap heating profile from the FM-TAS-I tests.

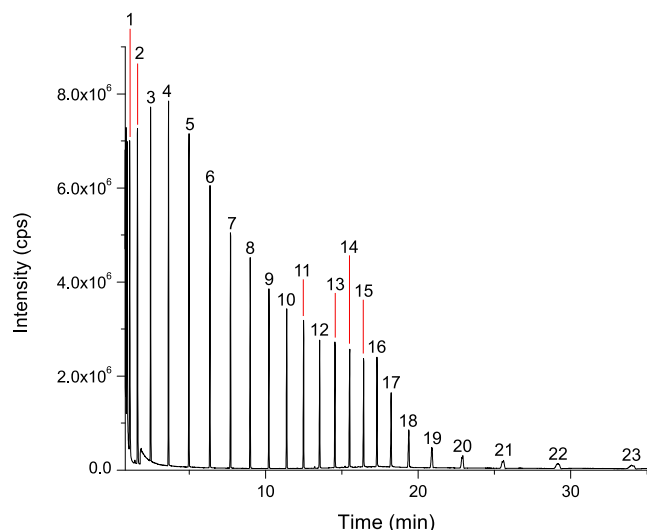**Fig. 3.** $C_7$–$C_{40}$ alkanes solution run on the MXT 5 column. The x-axis scale represents a nominal MOMA run time of 35 min. (1) heptane, (2) octane, (3) nonane, (4) decane, (5) undecane, (6) dodecane, (7) tridecane, (8) tetradecane, (9) pentadecane, (10) hexadecane, (11) heptadecane, (12) octadecane, (13) nonadecane, (14) icosane, (15) henicosane, (16) docosane, (17) tricosane, (18) tetracosane, (19) pentacosane, (20) hexacosane, (21) heptacosane, (22) octacosane, (23) nonacosane. The GC column was heated from 45 °C to 220 °C with a 10°C·min$^{-1}$ ramp and held for a total run time of 35 min.
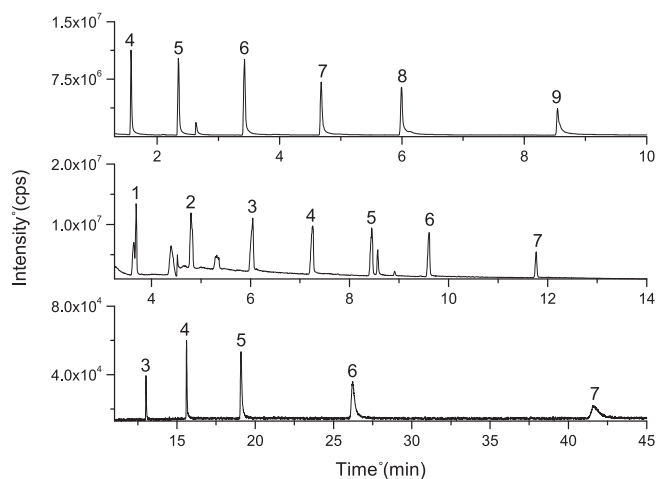


**Fig. 4.** A comparison of the separation capabilities of derivatized and non-derivatized alcohols on the MXT CLP and MXT Q BOND capillary columns. (Top) pure alcohols, MXT CLP, (Middle) MTBSTFA-derivatized alcohols, MXT CLP, and (Bottom) pure alcohols, MXT Q BOND. (1) ethanol, (2) 1-propanol, (3) 1-butanol, (4) 1-pentanol, (5) 1-hexanol, (6) 1-heptanol, (7) 1-octanol, (8)1-nonanol, (9) 1-undecanol. Although marked with the same numbering system, note that in the case of the middle panel, molecules are MTBSTFA-derivatized alcohols. The GC column was heated from 45 °C to 220 °C (MXT CLP) or 200 °C (Q BOND) with a 10°C·min$^{-1}$ ramp and held for a total run time of 35 min or 45 min.

allows the analysis of refractory and/or insoluble matter in complex matrices (Geffroy-Rodier et al., 2009). In this paper, we will not explore the use of TMAH for martian organic analyses because it has been covered recently in other publications (He et al., 2019).

Solid amino acids and carboxylic acids were diluted in demineralized water at a concentration of $10^{-2}$ mol·L$^{-1}$. 10 μL of these standard solutions were put into a 2 mL glass vial to evaporate the water under a stream of dry gaseous pure dinitrogen. 30 μL of MTBSTFA and 10 μL of DMF were added to the vial and the derivatization reaction took place by

heating the mixture at 75°C for 30 min (Millan et al., 2016). For the DMF-DMA derivatization, 20 μL of DMF-DMA were added to the vial containing the dried amino acid sample before heating the mixture at 140°C for 3 min (Freissinet et al., 2010). Derivatization was also performed on alcohol mixtures: 0.1 μL of each alcohol was diluted directly with the derivatization agent (40 μL MTBSTFA/DMF (4:1 mixing ratio); 20 μL DMF-DMA) before the derivatization heating protocol. 0.5 μL of the final solution were injected into the GC-MS.

For the derivatization that was performed directly on a solid natural sample (see 2.1.4 section) spiked with amino acids, 15 μL of DL-serine and DL-alanine, diluted in demineralized water at a concentration of $10^{-2}$ mol·L$^{-1}$ were added to 15 mg of the natural sample and placed under a stream of dry gaseous pure dinitrogen until complete evaporation of the water. 30 μL of DMF-DMA were then added and the solution was heated at 200°C for 3 min. The solution was then extracted, with some solid particles in the liquid extract, using a 100 μL liquid syringe (Hamilton) and centrifuged for 1 min to separate the solid and liquid parts. 1 μL of the supernatant was injected to the GC-MS using a 5 μL liquid syringe (SGE).

### 2.1.4. Natural analog sample

Enantiomeric resolution of DL-alanine and DL-serine was studied on a natural analog sample which was spiked with amino acids. The Arctic Mars Analog Svalbard Expedition (AMASE) KitKat sample, a buff-colored carbonate mudstone, was selected as the natural analog sample for this study. This sample is from an environment which has low levels of organic and biological material in mineralogical assemblages as well as a climate relevant to Mars. Carbonates have been found on Mars (Ehlmann et al, 2008; Morris et al, 2010) and in martian meteorites (McKay et al., 1996) and are good reservoirs for organics. Even if phyllosilicate-bearing terrains are expected at Oxia Planum, the now selected landing site for the Rosalind Franklin rover, a relevant Oxia Planum analog sample for laboratory testing still remains to be fully constrained (Poulet et al., 2019; Quantin et al., 2016) and additional minerals to those seen from orbit are likely to be detected *in situ* (Rampe et al., 2018). Additionally, since our objective is to test the capabilities of the MOMA flight spare columns within known MOMA operating conditions, we rely on previous MOMA testing which has been employed on this same sample (Siljeström et al., 2014).

### 2.2. Instrumentation

#### 2.2.1. Metallic capillary columns

Duplicates of the four MOMA capillary columns were used for this study. Each is one of the two duplicates of each column (three for the Chirasil Dex) purchased in 2013 in the same batch as the flight columns. After their purchase, the columns were tested with a limited number of compounds and the results were used to confirm the good health and performances of the columns during their integration into the flight hardware, and finally to select the ones for the flight and spare models of the instrument. After these tests, the non-selected columns were kept under clean storage conditions. They were plugged and stored in a plastic bag pressurized with pure dinitrogen (99.9999% purity from Linde). The original columns purchased were 25 m long. Due to mass constraints for the space instrument, each column was shortened to 20 m. Characteristics of each column are summarized in Table 2. This combination of four columns was chosen for the purposes of being able to separate a wide range of organic molecules, including i) volatile organic molecules containing 1 to about 25 carbon atoms, ii) organic enantiomers, iii) species produced from derivatization with the three chemical reagents to be used on MOMA, and iv) inorganic volatiles (Goesmann et al., 2017). The combination of these four types of columns (*i.e.*, a porous-layered open tubular (PLOT) column, a chiral wall-coated open tubular (WCOT) column, and two general purpose (WCOT) columns) fulfilled these requirements, while assuring some redundancy and overlap in their targeted compounds (as in Szopa et al., 2002, Szopa et al., 2004).
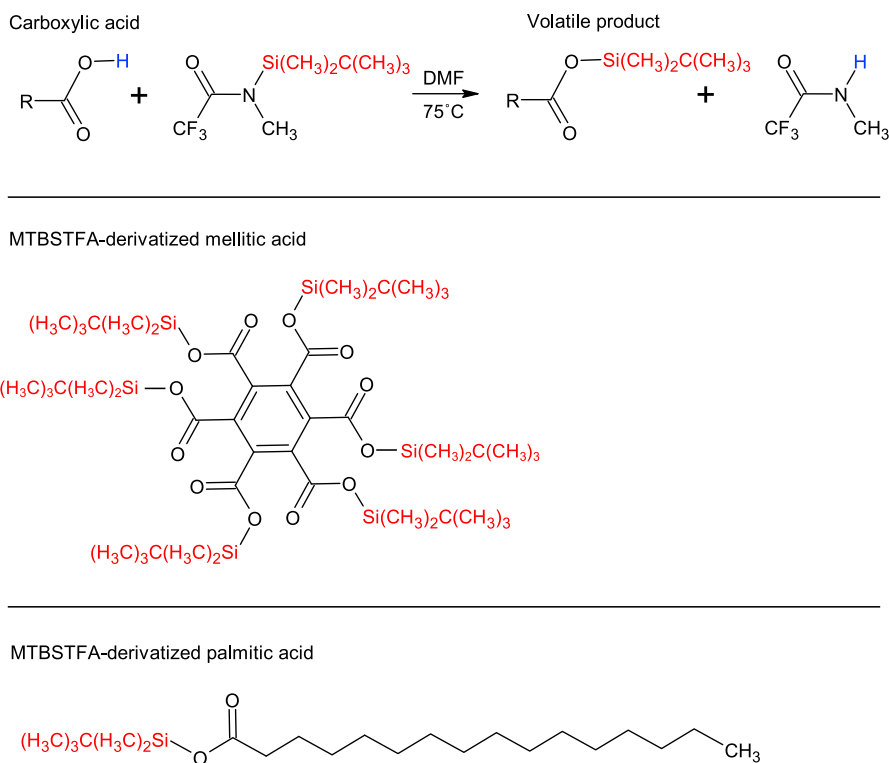
Carboxylic acid

Volatile product



MTBSTFA-derivatized mellitic acid



MTBSTFA-derivatized palmitic acid



**Figure 5.** (Top) Scheme of the chemical reaction between a carboxylic acid and MTBSTFA. (Middle) MTBSTFA-derivatized mellitic acid showing six carboxylic acid functions. Therefore, mellitic acid has six additional tert-butyldimethylsilyl groups added after derivatization with MTBSTFA, leading to a much higher molecular mass than (bottom) MTBSTFA-derivatized palmitic acid with only one carboxylic acid function and one additional tert-butyldimethylsilyl group.

### 2.2.2. Gas chromatography mass spectrometry run conditions

The measurements were carried out with a GC Trace Ultra coupled to an Ion Trap Quadrupole (ITQ) MS and a GC Trace Ultra or a GC Trace 1300 coupled to a Single Quadrupole MS (ISQ) (all from ThermoFisher Scientific). The same protocols were used for each instrument. The laboratory work was performed on ITQ/ISQ mass spectrometers, while MOMA will carry a linear ion trap (LIT) mass spectrometer which is a miniaturized version of the ThermoFisher LXQ design (Arevalo et al., 2015). However, the comparison between MOMA ETU data and laboratory data in Section 3.2.3 is sufficient since this current work is focused on the gas chromatography parameters, such as retention time and peak shape, which are not affected by any differences between an LXQ and ITQ/ISQ-type design. The laboratory MS data is used for the identification of compounds, which is also sufficient since all compounds which are injected and studied are known standards.

A split/splitless syringe injector (split ratio of 20 or 50) was used to vaporize and transfer the liquid samples to the column. The temperature of the injector was $250°C$ and the temperature of the GC-MS transfer line was $250°C$ to allow the volatilization of all the species studied and their transfer to the MS without any risk of condensation. The laboratory ITQ and ISQ instruments used in this study scanned the ions produced after electron impact ionization of the molecules at 70 eV from $m/z$ 10 to 500. The ionization source temperature was set at $250°C$. The carrier gas was helium (99.999% purity from Air Liquide), the same type of helium which is used in the MOMA FM.

On MOMA, the flow rate is adjustable from 0.8 mL·min$^{-1}$ to 1.4 mL·min$^{-1}$, with a nominal flow rate at about 1.2 mL·min$^{-1}$. The initial column temperature can be as low as $30°C$ and will be ramped to a final temperature which is dependent on a given column and limited either due to the maximum temperature of use of a column or to the limited amount of energy that can be used for heating. Due to these constraints,

the expected MOMA gas chromatographic run duration is about 35 min. Because there is adjustability to the parameters of flow rate and column temperature program, it is important to ensure that experiments will be completed in the shortest time possible on Mars without compromising chromatographic performance. For the study of standards on the columns, the GC column was heated from 45 to $220°C$ for the MXT 5 and MXT CLP columns, $45–180°C$ for the Chirasil Dex column, and $45–200°C$ for the MXT Q BOND column, with a $10°C·min^{-1}$ ramp in all cases. $220°C$ is shown to be the maximum column temperature which can be reached on the FM based on recent tests performed on a MOMA engineering test unit (ETU) similar to the FM (Section 2.2.3). 180 °C and 200 °C were chosen as the maximum operating temperatures for the Chirasil Dex and MXT Q BOND columns respectively, as they are 20 °C lower than the maximum temperature of the columns recommended by the suppliers. This difference was chosen to avoid a premature degradation of the columns' stationary phases. For the study of enantiomeric resolution of chiral molecules, the column was held at $35°C$ for 7 min, then heated to $182°C$ with a $10°C·min^{-1}$ or a $3°C·min^{-1}$ ramp. The column temperature programs used in our tests are shown in Fig. 1.

### 2.2.3. Relevant tests on MOMA ETU and FM

Our laboratory tests were performed on a commercial GC-MS system with a hand-held syringe injection. However, at points throughout the paper we will compare these laboratory analyses with tests performed on both an ETU and the FM. The two such testing campaigns that will be referred to in this paper are 1) tests performed during a GC-MS coupling campaign at the NASA Goddard Spaceflight Center (GSFC) on an ETU in 2018 (Kaplan et al., 2019), described in Section 3.2.3 and referred to as the ETU tests, and 2) thermal-vacuum tests on the FM performed at the Thales Alenia Space Italia (TAS-I) in 2019, referred to as the FM-TAS-I tests. Important differences between the laboratory and an ETU/FM

scenario include the method of sample injection, transfer line temperatures, and the gas sample processing system. Some quantitative operational information is given in Table 3 to summarize some of these differences. On MOMA, injection traps (IT), based on the principle of thermal desorption, allow direct transfer of compounds to the column. Trapped chemical species are released from the IT to the chromatographic columns by rapid heating (Fig. 1) to enable sufficiently short injection times (Goesmann et al., 2017). In the laboratory, injection is completed manually with a hand-held microliter-volume syringe.

# 3. Results and discussion

## 3.1. Separation power of selected standards

A number of chemically diverse compounds (Table 1) were targeted and tested on a laboratory GC-MS under constrained operating conditions imposed by the limitations of the space experiment. Alkanes, alcohols, carboxylic acids, and amino acids were tested on each of the appropriate spare MOMA GC columns. The retention time, or the time for each solute to pass through a given chromatographic column, of each compound by chemical family and by GC column are catalogued in Table 4 (Chirasil Dex, MXT 5 and MXT CLP columns) and Table 5 (MXT Q BOND column) and are also described pictorially in Fig. 7. This type of retention time library allows for an examination of the capability of the chromatographic column suite as a package to achieve the needed separations under MOMA-like operating conditions. We will develop with more details the performances of each chromatographic column.

### 3.1.1. MXT Q BOND

The MXT Q BOND column is dedicated to the separation of the lightest compounds including the noble gases and the smallest hydrocarbons. Although we cannot expect to elute any compound above a $C_6$ carbon chain with this column in a nominal 35-min run time, we will be able to clearly separate lighter organic compounds and even inorganic gases which are permanently gaseous under martian atmospheric conditions. Although the scientific priority of MOMA will be the detection of organic molecules in solid samples, our tests show that the noble gases can be successfully separated on the MXT Q BOND column (Fig. 2) using a lower carrier gas flow rate (1.0 mL·min$^{-1}$) and the ETU temperature program (Fig. 1). This is an example of additional science, *e.g. in situ* isotope measurements of noble gases in the martian atmosphere (Conrad et al., 2016), that can be successfully completed using the MOMA chromatographic column package with a modified column temperature program within the adjustability of MOMA.

### 3.1.2. MXT 5 and MXT CLP columns

The MXT 5 and MXT CLP columns were selected for the separation of organic compounds that contain up to about 25 carbon atoms (depending on their chemical nature). The number of compounds targeted by these columns is significant and the opportunity for overlap of a compound of interest with another peak coming from the martian sample and/or from derivatization products and byproducts is likely, given the complexity of most chromatograms from natural samples. Therefore, the use of two columns limits the risk of non-identification of such species (Szopa et al., 2002c; 2003). Moreover, most of the compounds we expect to detect should be analyzed with these columns. Their capability to separate the same range of compounds is therefore a key instrumental redundancy in the case that the performance of one of these columns is degraded through time on Mars. Fig. 7 illustrates how the retention times across families of molecules on each of these two columns is very similar, yet staggered, increasing the likelihood of detecting compounds of interest and creating redundancy within the GC subsystem.

Fig. 3 shows $C_7$–$C_{29}$ alkanes (up to $C_{40}$ were injected) detected on the MXT 5 column within the 35-min GC run time. An expected significant peak broadening is observed with increasing retention time, due to increased longitudinal diffusion inside the column. This broadening with

**Table 4**
Retention times of selected compounds on the Chirasil Dex, MXT 5, and MXT CLP columns. The measured dead times were 0.63–0.70 min (MXT 5), 0.69–0.76 (MXT CLP), and 0.61–0.63 (Chirasil Dex). *Shows a comparison between retention times for runs with a dead time of 0.69 vs. 0.63 min. **Less robust identification due to low mass spectra resolution at higher m/z values on the lab instrument. The range in dead time values was constrained by the operating range of each instrument.

| Family | Compound Reference Number | Compound | Chirasil Dex | MXT 5 | MXT CLP |
|---|---|---|---|---|---|
| Alcohols | 1 | 1-Propanol-1, pure | 1.53 | 0.84 | 0.95 |
| | 2 | 1-Butanol, pure | 2.91 | 1.03 | 1.19 |
| | 3 | 1-Pentanol, pure | 4.48 | 1.46 | 1.68 |
| | 4 | 1-Hexanol, pure | 5.78 | 2.24 | 2.48 |
| | 5 | 1-Heptanol, pure | 6.91 | 3.32 | 3.59 |
| | 6 | 1-Octanol, pure | 8.03 | 4.64 | 4.87 |
| | 7 | 1-Propanol, DMF-DMA derivative | 3.96 | 2.53 | 2.41 |
| | 8 | 1-Butanol, DMF-DMA derivative | 5.12 | 3.63 | 3.40 |
| | 9 | 1-Pentanol, DMF-DMA derivative | 6.43 | 4.92 | 4.57 |
| | 10 | 1-Hexanol, DMF-DMA derivative | 7.73 | 6.22 | 5.82 |
| | 11 | 1-Heptanol, DMF-DMA derivative | 8.97 | 7.54 | 7.06 |
| | 12 | 1-Octanol, DMF-DMA derivative | 10.16 | 8.77 | 8.27 |
| | 13 | 1-Propanol, tbdms | 6.49 | 2.66 | 2.62 |
| | 14 | 1-Butanol, tbdms | 7.79 | 3.78 | 3.55 |
| | 15 | 1-Pentanol, tbdms | 9.00 | 4.98 | 4.76 |
| | 16 | 1-Hexanol, tbdms | 10.15 | 6.29 | 5.98 |
| | 17 | 1-Heptanol, tbdms | 11.27 | 7.58 | 7.21 |
| | 18 | 1-Octanol-1, tbdms | 13.52 | 8.82 | 8.42 |
| Alkanes | 19 | Heptane ($C_7$) | 1.66 | 1.10 | 0.97 |
| | 20 | Octane ($C_8$) | 2.60 | 1.61 | 1.36 |
| | 21 | Nonane ($C_9$) | 3.85 | 2.47 | 2.05 |
| | 22 | Decane ($C_{10}$) | 5.23 | 3.64 | 3.06 |
| | 23 | Undecane ($C_{11}$) | 6.62 | 4.98 | 4.26 |
| | 24 | Dodecane ($C_{12}$) | 7.96 | 6.36 | 5.53 |
| | 25 | Tridecane ($C_{13}$) | 9.20 | 7.70 | 6.8 |
| | 26 | Tetradecane ($C_{14}$) | 10.38 | 9.00 | 8.04 |
| | 27 | Pentadecane ($C_{15}$) | 11.50 | 10.22 | 9.21 |
| | 28 | Hexadecane ($C_{16}$) | 12.57 | 11.39 | 10.34 |
| | 29 | Heptadecane ($C_{17}$) | 13.86 | 12.49 | 11.42 |
| | 30 | Octadecane ($C_{18}$) | 15.70 | 13.55 | 12.44 |
| | 31 | Nonadecane ($C_{19}$) | 18.43 | 14.55 | 13.41 |
| | 32 | Icosane ($C_{20}$) | 22.56 | 15.51 | 14.34 |
| | 33 | Henicosane ($C_{21}$) | 28.84 | 16.42 | 15.23 |
| | 34 | Docosane ($C_{22}$) | Not | 17.31 | 16.91 |
| | 35 | Tricosane ($C_{23}$) | within | 18.23 | 17.71 |
| | 36 | | run time | 19.39 | 19.8 |

*(continued on next page)*

**Table 4** (*continued*)

| Family | Compound Reference Number | Compound | Chirasil Dex | MXT 5 | MXT CLP |
|--------|---------------------------|----------|--------------|-------|---------|
| | | Tetracosane ($C_{24}$) | | | |
| | 37 | Pentacosane ($C_{25}$) | | 20.89 | 21.28 |
| | 38 | Hexacosane ($C_{26}$) | | 22.93 | 23.27 |
| | 39 | Heptacosane ($C_{27}$) | | 25.60 | 25.76 |
| | 40 | Octacosane ($C_{28}$) | | 29.14 | 29.12 |
| | 41 | Nonacosane ($C_{29}$) | | 33.98 | 33.63 |
| Carboxylic Acids | 42 | Oxalic acid, dimethyl ester | 5.02** | 3.25** | 3.82** |
| | 43 | Benzoic acid, methyl ester | 6.93 | 5.49 | 5.47 |
| | 44 | Decanoic acid, methyl ester | 9.78 | 8.51 | 8.25 |
| | 45 | Dodecanoic acid, methyl ester | 12.02 | 11.01 | 10.55 |
| | 46 | Palmitic acid, methyl ester | 20.19 | 14.81 | 14.55 |
| | 47 | Mellitic acid, DMF-DMA derivative | Not within run time | | |
| | 48 | Oxalic acid, di-tbdms | 11.76** | 11.30 | 10.93** |
| | 49 | Benzoic acid, tbdms | 11.31 | 10.56 | 10.28 |
| | 50 | Decanoic acid, tbdms | 13.55 | 12.31 | 12.22 |
| | 51 | Dodecanoic acid, tbdms | 17.67 | 14.43 | 14.02 |
| | 52 | Palmitic acid, tbdms | 26.88 | 18.19 | 17.50 |
| | 53 | Mellitic acid, MTBSTFA derivative | Not within run time | | |
| Amino Acids | 54 | DL-Serine, DMF-DMA derivative | 6.93, 7.20 | 4.26/ 3.90* | 4.79 |
| | 55 | Glycine, DMF-DMA derivative | 8.00 | 6.57 ($t_M$ = 0.69 min) | 6.85 |
| | 56 | DL-Alanine, DMF-DMA derivative | 7.41, 7.63 | 6.62 ($t_M$ = 0.69 min) | 6.63 |
| | 57 | DL-Valine, DMF-DMA derivative | 8.62, 8.69 | 8.10/ 7.59* | 7.95 |
| | 58 | DL-Leucine, DMF-DMA derivative | 9.68, 9.71 | 9.30/ 8.78* | 9.05 |
| | 59 | DL-Glutamic Acid, DMF-DMA derivative | 13.08 | 11.87 ($t_M$ = 0.63 min) | 12.55 |
| | 60 | DL-Serine, MTBSTFA derivative | 14.31** | 13.30 | 13.10** |
| | 61 | Glycine, MTBSTFA derivative | 12.10 | 10.90 | 10.72 |
| | 62 | DL-Alanine, MTBSTFA derivative | 11.53 | 10.61 | 10.46 |
| | 63 | | 12.66 | 11.94 | 11.71 |

**Table 4** (*continued*)

| Family | Compound Reference Number | Compound | Chirasil Dex | MXT 5 | MXT CLP |
|--------|---------------------------|----------|--------------|-------|---------|
| | | DL-Valine, MTBSTFA derivative | | | |
| | 64 | DL-Leucine, MTBSTFA derivative | 13.17 | 12.41 | 12.18 |
| | 65 | DL-Glutamic Acid, MTBSTFA derivative | 19.82 | 15.37 | 15.12 |

**Table 5**

Retention times for selected compounds on the MXT Q BOND column. The measured dead time was ~0.55 min. *The ETU temperature program was used.

| Family | Compound Reference Number | Compound | Q-PLOT |
|--------|---------------------------|----------|--------|
| Alcohols (pure) | 1 | 1-Propanol | 10.11 |
| | 2 | 1-Butanol | 13.02 |
| | 3 | 1-Pentanol | 15.61 |
| | 4 | 1-Hexanol | 19.09 |
| | 5 | 1-Heptanol | 26.21 |
| | 6 | 1-Octanol | 41.56 |
| Noble Gases (pure) | 66 | Neon | 0.85* |
| | 67 | Argon | 0.89* |
| | 68 | Krypton | 0.98* |
| | 69 | Xenon | 1.69* |
| Hydrocarbons (pure) | 70 | Ethane | 1.13 |
| | 71 | Ethylene | 0.95 |
| | 72 | Butane | 6.38 |
| | 73 | Pentane | 9.61 |

increasing molecular weight has consequences for the detection limit of higher molecular weight compounds. In tests performed on the MXT CLP in which $C_7$–$C_{40}$ alkanes were injected, up to a $C_{30}$ alkane was visible above background at a retention time of about 40.10 min (longer than a nominal MOMA run) before the signal was no longer resolvable from the background signal. Our tests demonstrate a best-case scenario in terms of the maximum carbon number (in this case, for alkanes) that will be detectable by MOMA. First of all, we start the GC temperature ramp immediately with no isothermal hold at the beginning of the run; conversely, on MOMA and flight-like setups such as the ETU, there is an isothermal hold of at least 1–5 min at the beginning of the GC run, both to elute non- and poorly-retained compounds and to accommodate time for trap cooling/flow path changes prior to the start of the ramp. In addition, it has not yet been systematically characterized how differences in the operating temperatures (e.g. line temperature differences) and gas processing systems between the FM and the laboratory (Table 3) will affect the maximum carbon number we could expect to see with MOMA.

As described in the introduction, compounds that contain a labile polar functional group, such as the alcohols, amino acids, and carboxylic acids, require derivatization in order to be reliably identified by a GC-MS system. Based on the relative retention time results for these three families of compounds (Fig. 7), the MXT CLP column appears to have a more polar stationary phase, since molecules with higher polarity such as the pure alcohols are slightly more retained by the MXT CLP than for the MXT 5 column. Additionally, the alkane group, with the least polarity, is retained by the stationary phase of the MXT 5 slightly longer than for the MXT CLP. When molecules (*i.e.* alcohols, carboxylic acids, amino acids) are derivatized and become less polar, the compounds often elute first from the MXT CLP column, meaning they experience a weaker interaction with the stationary phase.

$C_3$ to $C_8$ linear alcohols were injected and were detected in their pure, DMF-DMA derivatized, and MTBSTFA derivatized forms. Fig. 4 shows a comparison between the retention times of pure alcohols and with
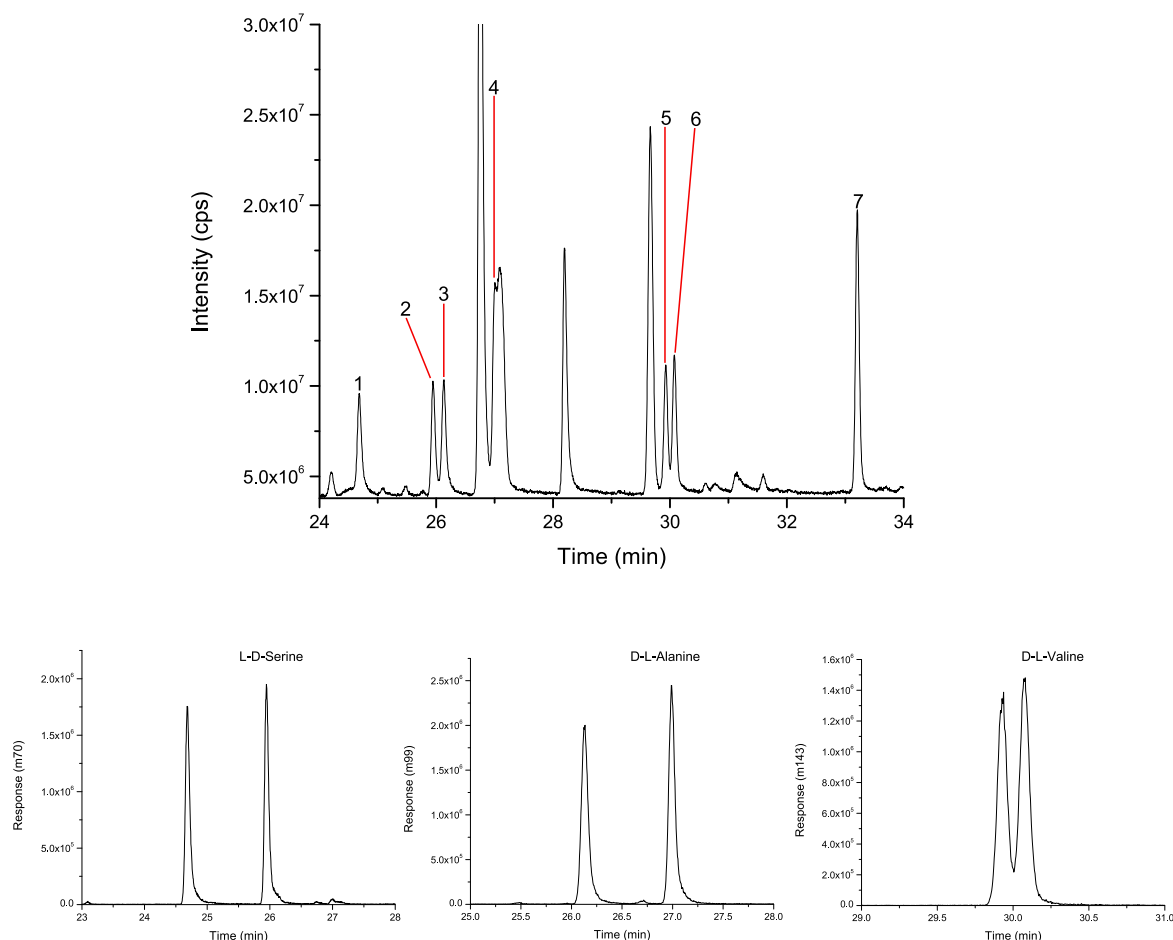
**Fig. 6.** (Top) DMF-DMA derivatized amino acids separated on the Chirasil Dex column. (1) L-serine, (2) D-serine (3) D-alanine, (4) L-alanine (5) DMF-DMA byproduct, (6) glycine, (7) DL-serine*, (8) D-valine, (9) L-valine (10) DL-leucine. (Bottom) A magnification of the above chromatogram showing the separation of DL-serine, DL-alanine, and DL-valine. The GC column was held at 35 °C for 7 min, then heated to 182 °C with a 3°C·min$^{-1}$ ramp. DL-glutamic acid was detected at a retention time of 44 min, and was not enantiomerically separated, but is not plotted here so that the separation of other enantiomers is clearly visible. *All the mass spectra of the derivatized amino acids, including L-D-serine, follow Freissinet et al. (2010) Table 1. Peak 7 is an additional DMF-DMA derivative of DL-serine, possibly DL-serine, -dimethyl, -methyl ester.

MTBSTFA derivatization on the MXT CLP column and pure alcohols separated by the MXT Q BOND column. This comparison illustrates two important components of the gas chromatography analysis. First of all, when derivatization is performed, especially in the case of MTBSTFA derivatization in which a silyl group $(Si(CH_3)_2C(CH_3)_3)$ replaces any labile hydrogen, the mass of the compound can increase substantially. This accounts for the higher retention times of derivatized compounds in Fig. 4 on the MXT CLP column and will be an important consideration when adjusting for GC run time during derivatization runs on Mars. It is particularly interesting for the case of the derivatized alcohols because the retention time for alcohols derivatized with MTBSTFA versus with DMF-DMA is quite similar for the MXT 5 and MXT CLP columns (Fig. 7). This suggests that the DMF-DMA derivatized alcohols are not merely undergoing a methylation, but rather a dimethylformamidination or another closely related reaction, causing the mass of the parent alcohol molecule to increase proportionally to the mass of an added silyl group. This example illustrates the importance of understanding the potential mass spectral library for MOMA surface science in addition to the retention time library fully described in this paper. Secondly, a comparison between alcohols separated by the MXT CLP, a WCOT column, and the MXT Q BOND, a PLOT column, shows the expected higher retention times produced by a PLOT column compared with a WCOT

column since PLOT columns have a thick porous layer of adsorbent attached to the column walls which increases the amount of time in which compounds interact with the stationary phase. In Fig. 4, the decreasing baseline level is due to peak broadening with increasing retention time, due to increased longitudinal diffusion inside the column.

All of the studied derivatized aromatic and aliphatic carboxylic acids were detected (up to hexadecanoic acid (palmitic acid), *m/z* 256), except mellitic acid (*m/z* 342). While the molar mass of hexadecanoic acid is about 256 g·mol$^{-1}$, it has only one carboxylic acid function, while mellitic acid has six carboxylic acid functions (Fig. 5). Therefore, mellitic acid has six additional *tert*-butyldimethylsilyl groups added after derivatization with MTBSTFA, which leads to a molecular mass of 1026 g·mol$^{-1}$. This explains the non-detection of mellitic acid in comparison to the detection of hexadecanoic acid within the nominal MOMA GC run time. Given the elution time of hexadecanoic acid on the MXT 5/CLP and the Chirasil Dex columns, it is likely that a linear carboxylic acid with a molecular mass of around 340 g·mol$^{-1}$ and only one labile hydrogen, corresponding to a molecular mass of only around 454 g·mol$^{-1}$ after MTBSTFA derivatization, would be visible within the nominal MOMA GC run time. Although the run time did not allow the detection of mellitic acid, several potential byproducts of mellitic acid were observed after derivatization by DMF-DMA on the MXT 5 column, *e.g.* 1,2,4-benzenetricarboxylic acid,
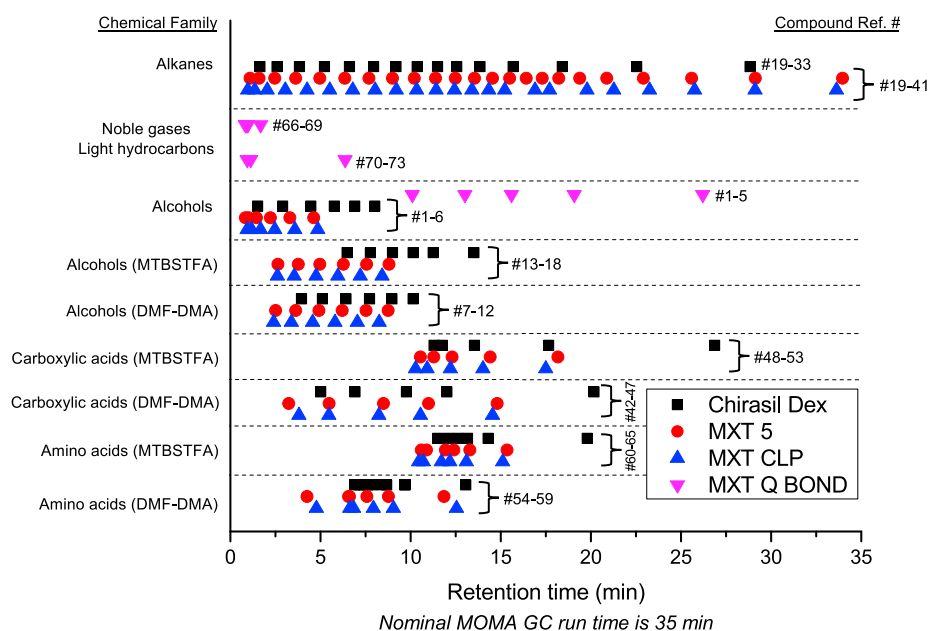
**Fig. 7.** An illustration of the spread of retention times of tested compounds across a nominal 35-min gas chromatographic run for each of the MOMA GC columns. The Compound Ref. # corresponds to the values given for each compound in Tables 4 and 5.

trimethyl ester and 1,2-benzenedicarboxylic acid bis(2-methylpropyl) ester. It is easier to detect partially derivatized mellitic acid with DMF-DMA in comparison with MTBSTFA, because adding a methyl group to the molecule (DMF-DMA) in comparison to a tert-butyldimethylsilyl group (MTBSTFA) results in a lower molecular weight of the final molecule after derivatization, which means a greater chance of it eluting during the 35-min run.

*3.1.3. Chirasil Dex column*

We cannot retrieve up to the same molecular weight compounds with the Chirasil Dex column, in comparison to the MXT 5/CLP columns, since the maximum operating temperature allowed for the integrity of the column's stationary phase is lower. However, the Chirasil Dex column has the obvious added value of enabling enantiomeric separation. We study enantiomeric resolution of amino acids and other chiral molecules on the MOMA chiral column in more detail in Section 3.2.1. Additionally, the Chirasil Dex column appears more polar than either the MXT CLP or the MXT 5, since polar compounds such as the pure alcohols have the longest retention times of these three columns. Therefore, this column will also have better separation of more polar molecules. The retention times for derivatized carboxylic acids are higher on the Chirasil Dex column than the MXT series for both MTBSTFA and DMF-DMA derivatization. The molecules have become less polar after derivatization, but it appears that other physical and/or chemical interactions between these specific kinds of molecules, *i.e.* amino acids and carboxylic acids, and the stationary phase of the Chirasil Dex column are also important.

All of the injected derivatized amino acids were detected (i.e. DL-serine, DL-alanine, glycine, DL-valine, DL-leucine, and DL-glutamic acid). The chiral enantiomers of L-D-serine, D-L-alanine, and D-L-valine were separated under run conditions similar to those performed during the ETU tests (Fig. 6). As described in Section 2.1.3, the –COOH group of the amino acid is methylated while the amine group undergoes dimethylformamidination during the DMF-DMA derivatization reaction. Additional derivatization can also occur on –OH groups attached to the side chain. An example of this is DL-serine, which has an additional hydroxyl group and therefore will undergo additional derivatization. The MTBSTFA-derivatized serine will undergo trisilylation, which has a clear effect on the final molecular weight of the compound and its retention

time (Fig. 7, Table 4). The later retention times of derivatized amino acids on the Chirasil Dex as compared to those on the MXT series is not as pronounced as for other molecules, with the exception of DL-serine, likely due to its polar quality and its resulting derivatization process.

*3.1.4. Combined effectiveness of MOMA chromatographic column package*

A full table of retention times is shown in Table 4 (Chirasil Dex, MXT 5, MXT CLP) and Table 5 (MXT Q BOND). The separation domains of the columns overlap and most of the targeted volatile species are detectable by the GC column package, demonstrating the system to be efficient for the separation of compounds in the same mass range than those originally targeted by MOMA. Fig. 7 illustrates the overlapping separation domains of the GC column package with a cartoon that visually summarizes the spread of retention times of targeted compounds across a 35-min run time. Species identification by the flight chromatograms will require the availability of this type of database and likely will require iterations on systematic laboratory tests such as this one. These tests do not consider the capabilities of the MOMA hydrocarbon traps, which may limit heavier molecules from ever reaching the column, since the temperature controls of the hydrocarbon traps can be optimized to adsorb/desorb compounds within a specific range of number of carbon atoms. Molecules which are not desorbed from the hydrocarbon trap during injection may still be detected by the MOMA LDMS. If preliminary biomolecules are detected on Mars, flight and laboratory GC-MS runs will inform the trade space on whether to modify the GC run conditions in order to target higher molecular weight compounds. Conversely, if the team wants to focus on the separation of small molecules, the temperature ramp could be decreased.

In addition to eluting across a range of retention times, the types and families of molecules were chosen in order to assess the separation of important compounds for MOMA's science objectives which include testing for bioindicators and biosignatures. For example, many important biochemicals exist in discreet molecular weight ranges (*e.g.*, $C_{14}$–$C_{20}$ lipid fatty acids). Whereas the relative abundance for abiotic volatiles in cosmic carbon chemistry is uniform and drops off as the carbon number increases (Ehrenfreund and Cami, 2010; Ehrenfreund and Charnley, 2000), the molecular weight distribution of biologically-derived matter is concentrated in discreet clumps corresponding to the various

life-specialized families of molecules (Summons et al., 2008). Additionally, many biological products (*e.g.*, proteins and nucleic acids) are synthesized from a limited number of simpler units. An identifiable molecular weight signature could be recovered in fragments from highly derived products, since classes of biomolecules can exhibit characteristic carbon chain length patterns. For example, $C_{15}$, $C_{20}$, $C_{25}$ carbon chain length patterns are constructed by acyclic isoprenoids using repeating $C_5H_{10}$ subunits and $C_{14}$, $C_{16}$, $C_{18}$, $C_{20}$ carbon chain length patterns are constructed by enzymes synthesizing fatty acids in $C_2H_4$ subunits (Vago et al., 2017). Our study suggests that the combination of pyrolysis and derivatization-GC-MS techniques on MOMA could enable the detection of $C_{29}$ straight-chain alkanes, $C_{20}$ straight-chain alcohols, as well as $C_{18}$ to $C_{20}$ straight-chain carboxylic acids, and $C_8$ or $C_{10}$ amino acids, depending on the derivatization reagent and the number of labile hydrogens. Therefore, the MOMA gas chromatographic columns would be capable of detecting straight-chain lipids in the form of alkanes, alcohols, and fatty acids with specific carbon patterns which indicates certain kinds of bacteria and plant life on Earth.

We also show that an assortment of proteogenic amino acids can be detected with the chromatographic column package, and that the column package enables multiple kinds of biosignature detection, including amino acid enantiomeric excess (which will be discussed in Section 3.2) and the relative abundance of types of amino acids. Biotic and abiotic processes on Earth can produce distinctly different amino acid (and lipid hydrocarbon) mixtures. Terrestrial life is selective, using a limited subset of molecular building blocks to construct larger, more complex biomolecules in order to meet physiological needs (Ehrenfreund et al., 2001; Eigenbrode, 2008; Summons et al., 2008). In contrast, abiotic processes favor random synthesis of smaller, simpler molecules (Davila and McKay, 2014; Georgiou, 2014). If subsurface Mars is sterile, amino acids and lipid hydrocarbons are still expected to be present given their abundance in meteorites, comets, synthesis products of hydrothermal reactions, and predicted products of organic chemistry models. The ability of the MOMA gas chromatographic column package to test multiple parameters (*e.g.*, relative abundance of amino acids, enantiomeric excess, patterns in lipid hydrocarbons, chain length distributions as a function of carbon number) enables a confidence value to any potential biosignature detection (Vago et al., 2017).

### 3.1.5. Comparison with Curiosity's SAM

Based on the vast experience of the Curiosity rover's SAM instrument, MOMA was designed to support the detection of higher mass compounds within chemical families of interest. The nominal flow rate is lower on SAM (~0.8 mL·min⁻¹) than on MOMA (~1.2 mL·min⁻¹) and the GC columns on SAM are longer, resulting in more retained compounds with longer retention times. For example, of the amino acids, only glycine and alanine are visible within SAM conditions from laboratory experiments, while we show here that MOMA run conditions allow for the detection of serine, valine, leucine, and glutamic acid in addition to glycine and alanine. On the alkane side, dodecane takes 18–20 min to elute from the SAM columns, while here we measure the retention time of dodecane to be between 5 and 8 min depending on the MOMA column (Millan et al., 2016). This comparison offers an exciting prospect for MOMA's capability to detect higher molecular weight compounds of interest on Mars.

### 3.2. Enantiomeric capability of MOMA's chiral column

### 3.2.1. Separation power

The MOMA instrument has the unique capability to detect and separate molecular enantiomers. The quantification of enantiomeric excess could reveal information about whether martian molecules are racemic or if they express an enantiomeric bias as is observed in terrestrial biomolecules. Therefore, it is paramount that a combination of the flight hardware, *i.e.* the gas chromatographic columns, the wet chemistry protocol, and the *in situ* operating conditions of the flight experiment, be shown to successfully separate chiral molecules into their enantiomers.

The resolution of both enantiomers, $R_S$, is used to characterize the degree of separation of two enantiomeric peaks, where:

$$R_S = 1.8 \cdot (t_R^B - t_R^A)/(\omega_A + \omega_B) \qquad \text{(Eq 1)}$$

$R_S$, the enantiomeric resolution, depends on two parameters, the time separating the two peaks (thermodynamic factor), $t_R^B$-$t_R^A$, and the width of each of the two peaks (kinetic factor), $\omega_A + \omega_B$. We tested the enantiomeric resolution of three types of chiral compounds: an alkane (3-methylheptane), underivatized alcohols (2-butanol, 2-pentanol, and 2-hexanol) and DMF-DMA derivatized amino acids (DL-serine, DL-alanine, DL-valine, DL-leucine, and DL-glutamic acid) as a function of the carrier gas velocity which moves solutes through the GC column.

The range of carrier gas velocities utilized for the study of enantiomeric resolution, and plotted in Fig. 8 (~40-80 cm·s⁻¹), corresponds to a range in dead time (the time for a non-retained compound to travel through the column) of ~0.45–0.85 min, consistent with the expected dead times on MOMA (Fig. 1). Fig. 6 shows the enantiomeric separation of L-D-serine, D-L-alanine, and D-L-valine on the MOMA spare chiral column and Fig. 8 shows the enantiomeric resolution of all the chiral compounds that were tested in this study. We find that "mid-range" (55-60 cm·s⁻¹) to "low" (35-55 cm·s⁻¹) helium velocities are optimal for enantiomeric resolution. For the alcohols, there is a decrease in resolution also at "low" flow rates (below ~55 cm·s⁻¹) with the exception of 2-butanol. We also find that baseline separation (separation at or below half-height-half-width of the chromatographic enantiomeric peaks) is achieved for most of the chiral compounds using a column temperature ramp of $10°C$·min⁻¹, a ramp which will allow for detection of higher molecular weight compounds within a given run time.

However, for the amino acids, baseline separation was achieved with a 10°C·min⁻¹ column temperature ramp only for DL-alanine and DL-serine. A lower temperature ramp, 3°C·min⁻¹, was employed, since lower temperature ramps have been shown to successfully separate amino acids after optimization on a longer (30 m) Chirasil Dex column (Freissinet et al., 2010). This lower temperature ramp allowed for baseline separation of an additional amino acid in our test set, DL-valine. Valine was not separated to half-height-half-width with the higher ramp rate, 10°C·min⁻¹. The optimization of enantiomeric separation is a tradeoff with run time, as the slower ramp requires longer run times and more resources from the spacecraft. MOMA has the capability to decrease its GC column temperature ramp as low as 1°C·min⁻¹. However, the implications of a lower ramp are that heavier molecules may not be detected during the run time.

### 3.2.2. Enantiomeric separation on natural sample

We tested a martian analog sample on the MOMA chiral column to demonstrate GC separation and identification of selected spiked amino acids in the presence of a complex mineral phase. As with the study of standards, we aim to test GC separation under conditions similar to that of the MOMA experiment without mimicking the entire process. For example, we performed derivatization in an oven external to the GC-MS instrument and then injected the derivatized sample by syringe injection, while for MOMA, the sample is heated within the oven until the derivatization reagent is released at a given temperature. However, the use of an analog sample allows the analysis of a more realistic gaseous mixture than those produced with chemical standards. Additionally, we can confirm that the influence of the mineral phase does not limit the ability to detect certain organic molecules such as amino acids if they are present at a certain concentration in the sample. The natural sample used in this study was spiked with amino acids, so that the amino acids were partially adsorbed to the sample's mineral matrix. On MOMA, thermal desorption performed on the sample prior to the release of the derivatization reagent will aid extraction of organics adsorbed on mineral surfaces and/or within interlayer spaces (Goesmann et al., 2017, Buch et al., 2009). We chose a derivatization temperature of 200 °C, consistent with the 175 °C temperature used during the AMASE campaign on the same
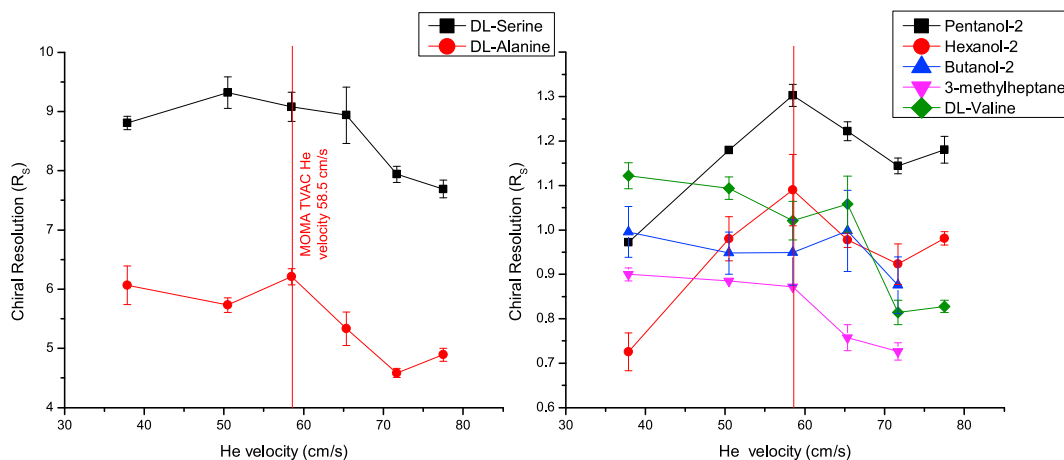
**Fig. 8.** Enantiomeric resolution of selected compounds vs. carrier gas linear velocity. 2-butanol and 3-methylheptane were not separated to baseline at the highest carrier gas velocity. The chiral alcohols and 3-methylheptane in this study are not derivatized while the amino acids are derivatized with DMF-DMA. The GC column was heated from 45 °C to 180 °C with a 3°C·min$^{-1}$ ramp for the amino acids and the GC column was heated at 35 °C for 7 min and ramped to 182 °C at a ramp rate of 10°C·min$^{-1}$ for the chiral alcohols and the 3-methylhexane.

sample (Siljeström et al., 2014). We select a higher temperature for the laboratory tests in order to procure a more efficient extraction of organics, but low enough to safeguard against decomposition of the derivatization reagent.

Fig. 9 shows the separation of enantiomers after DMF-DMA derivatization within a more complex natural sample. Comparing the enantiomeric behavior in Figs. 6 and 9 illustrates the appropriateness of

analog samples for limit of detection studies due to the more realistic noise levels. We expect to see peaks from other organic molecules indigenous to the sample, in addition to the spiked amino acids, since the AMASE KitKat sample was previously determined to contain low amounts of aliphatic and aromatic organic material after GC-MS pyrolysis and derivatization (Siljeström et al., 2014), although the enantiomers of amino acids indigenous to the sample have not been successfully
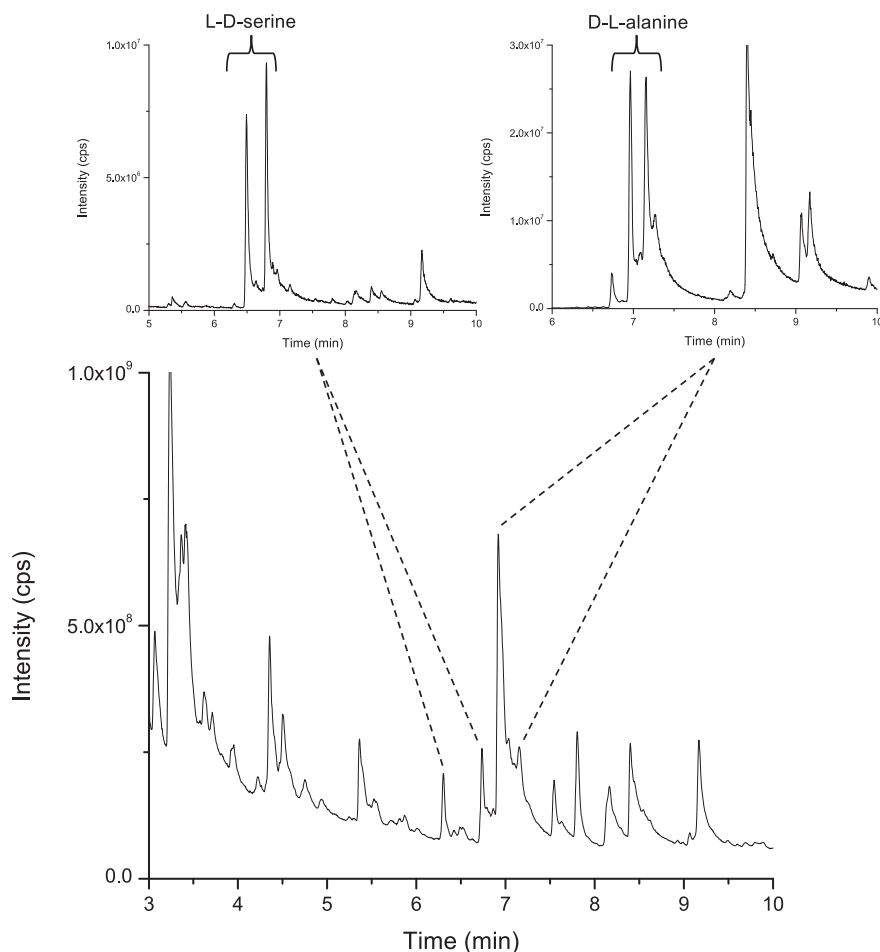


**Fig. 9.** Chromatogram resulting from the GC-MS analysis of the AMASE KitKat sample, spiked with amino acids and derivatized with DMF-DMA, on the MOMA Chirasil Dex column. (Bottom) Total ion current; (Top Left) extracted ion chromatogram for *m/z* 70, showing the enantiomers of L-D-serine; (Top Right) extracted ion chromatogram for *m/z* 99 showing the enantiomers of D-L-alanine. The GC column was heated from 45 °C to 180 °C with a 10°C·min$^{-1}$ ramp and held for a total run time of 35 min.

separated. The chromatograms in Fig. 9 illustrate the value of GC-MS instrument coupling for strict identifications of targeted compounds on these more realistic samples. On the chromatographic side, additional peaks with the same important ion fragments (*i.e. m/z* 70 and *m/z* 99) are prevalent in the single ion mode, sometimes at higher abundances than the targeted molecules themselves. On the mass spectrometry side, the occurrence of co-eluting peaks interferes with discreet mass spectral signatures and definitive identification by spectral libraries. The identification of DL-serine and DL-alanine were made using specific peak ions (*m/z* 70 and *m/z* 99 respectively) coupled with the known retention time of DL-serine and DL-alanine (measured by chemical standard in Section 3.1) which allows for the strict identification of these targeted chemical species. This exercise demonstrates the utilization of retention time libraries such as the one described in this paper in order to make identifications within more complex samples.

### 3.2.3. Comparison of enantiomeric separation between laboratory and MOMA ETU

Chiral molecules were recently analyzed on a MOMA ETU GC-MS coupled system at the NASA GSFC (Kaplan et al., 2019). A chiral compound, *i.e.* 3-methylhexane, has been consistently used in MOMA experiments as a reference compound. Here we use 3-methylhexane as a reference compound for comparing retention times under similar column temperature programs between the ETU tests and the laboratory. We also compare the enantiomeric separation results for DL-serine between the ETU tests and our laboratory results.

On the MOMA ETU (as on the FM), the MOMA injection trap is heated for at least 10–15 s in order to release organics adsorbed onto the trap material (Goesmann et al., 2017). Therefore, unlike in the laboratory, there is a minimum 10–15 s interval ambiguity to the exact injection time of a given compound. For our comparison between the ETU tests and the laboratory tests, we use the completion of the trap heating to calculate the lower limit of the retention time of 3-methylhexane on the MOMA ETU (Fig. 10). A retention time of 2.5 min is calculated for 3-methylhexane (ETU), which is consistent with a retention time of 2.4 min for 3-methylhexane (spare Chirasil Dex column, laboratory GC-MS) under the same GC temperature program (column held isothermally at 35 °C). Additionally, Fig. 10 compares the enantiomeric separation of DL-serine between the ETU test and a laboratory test with a similar GC column temperature program (ETU temperature curve in Fig. 1). For the ETU test, the GC column was held isothermally at 40 °C for 2.15 min, ramped at 10°C·min$^{-1}$ to ~182 °C and held for about 7.8 min. For the laboratory tests, the GC column was held at 35 °C for 7 min and then ramped at 10°C·min$^{-1}$ to 182 °C. This roughly 5-min difference in the initial isothermal hold is reflected in the roughly 5-min difference in retention times of serine between the laboratory and ETU tests (Fig. 10). This kind of comparison validates the value of a retention time library from laboratory tests for aiding compound identification on MOMA flight-like data sets.

In the ETU tests, the peak width of the 3-methylhexane peak (*m/z* 43) was 0.17 min, while in the laboratory tests, the peak width was 0.05 min (Fig. 10). Likewise, the enantiomeric peaks of L-D-serine (*m/z* 70) are broader in the ETU tests, about 0.14–0.20 min (ETU) compared with 0.028 min (laboratory). As defined in Equation (1), the distance separating the two enantiomeric peaks is also important for calculating enantiomeric resolution. Differences in this value between the ETU and laboratory may be explained by a difference in the method for controlling the flow rate as well as some ambiguity in selecting the peak center due to the asymmetric peak shape in the ETU case. A more efficient (sharper), symmetric peak in the laboratory results is consistent with the fast injection allowed by a syringe injection, the most efficient injection method for our given gas chromatography setup. The broader, slightly-tailing peaks in the ETU results are consistent with injection by adsorption/thermal desorption traps, in which the injection is less controlled and can be considered as a worst case. The difference between enantiomeric separation performed on a laboratory instrument versus in a MOMA ETU

setting illustrates the challenge of resolving enantiomers on Mars. However, a column's ability to resolve enantiomers is determined by its ability to separate enantiomeric peaks to half height. Separation at or below the half height of a peak is chromatographically considered a baseline separation. Although the implementation of enantiomeric separation for MOMA will undergo additional optimization on ETU and laboratory models before MOMA lands on Mars, these initial ETU tests show a successful baseline separation of the enantiomers of an amino acid.

As discussed in Section 3.1.4, amino acid enantiomeric excess is a detectable biosignature enabled by the enantioselective column on MOMA. Even though amino acid homochirality can serve as an important biosignature, recent measurements of l-enantiomeric excess values for some conglomerate-forming a-H proteinogenic amino acids on fragments of the Tagish Lake meteorite (Glavin et al., 2012) show that nonbiological processes could also lead to significant enantioenrichment for some amino acids. Additionally, a full study of the potential for racemization of chiral mixtures within instrument elements (*e.g.*, the heating protocol of the hydrocarbon traps) is required to rule out any important instrument influence on amino acid enantiomeric excess results. Both of these examples emphasize the need for multiple chemical channels of observations in order to establish confidence values for the biotic or abiotic nature of collected martian samples (Vago et al., 2017).

## 4. Conclusions

As we prepare for the launch and landing of the Rosalind Franklin rover, the work performed in this present study evaluates the performance of the four different gas chromatographic capillary columns coming from the same batch as those integrated in the FM. This work establishes a database of the retention times and mass spectra of the most probable organic compounds on Mars based on influx from the interplanetary medium, potential hydrothermal systems, atmospheric synthesis, and/or biological origins. This database is a necessary tool in order to robustly make identifications of target compounds within flight data. This symbiotic relationship between laboratory and flight data for enabling the strict identifications of target species has been previously demonstrated through the detection and identification of compounds using the SAM instrument and associated laboratory experiments (Eigenbrode et al., 2018; Freissinet et al., 2015; Millan et al., 2016; Szopa et al., 2020).

Following the finalization and delivery of the MOMA flight model, this study helps to redefine the constraints of the space instrument, since it is understood that space instrumentation is far less performant than traditional laboratory instrumentation and protocol. For example, we demonstrate the more performant separation of the enantiomers of L-D-serine in the laboratory versus in an ETU setting due to a more efficient injection by syringe (laboratory) rather than by adsorption/thermal desorption traps (space experiment). However, this study also serves to propose protocol which can improve the separation of compounds and the likelihood of a strict identification. For example, in the case of the separation of the enantiomers of amino acids, lower temperature ramps and flow rates are required. Since these conditions require more energy resources from the spacecraft, plans for decision trees during Mars operations will need to consider these requirements in order to meet science objectives.

In addition to the difference in performance between the flight experiment and the laboratory, the number of peaks and the level of complexity of a chromatogram obtained from the pyrolysis and/or derivatization of a martian sample, which includes the presence of a mineral matrix, is significantly greater than those obtained through the injection of chemical standards. We tested a natural sample spiked with amino acids in order to observe the effect of the presence of a mineral phase on the complexity of the chromatogram and the ability to resolve specific enantiomers in a scenario with more realistic background. The coupling of the chromatographic system with preparative wet chemistry
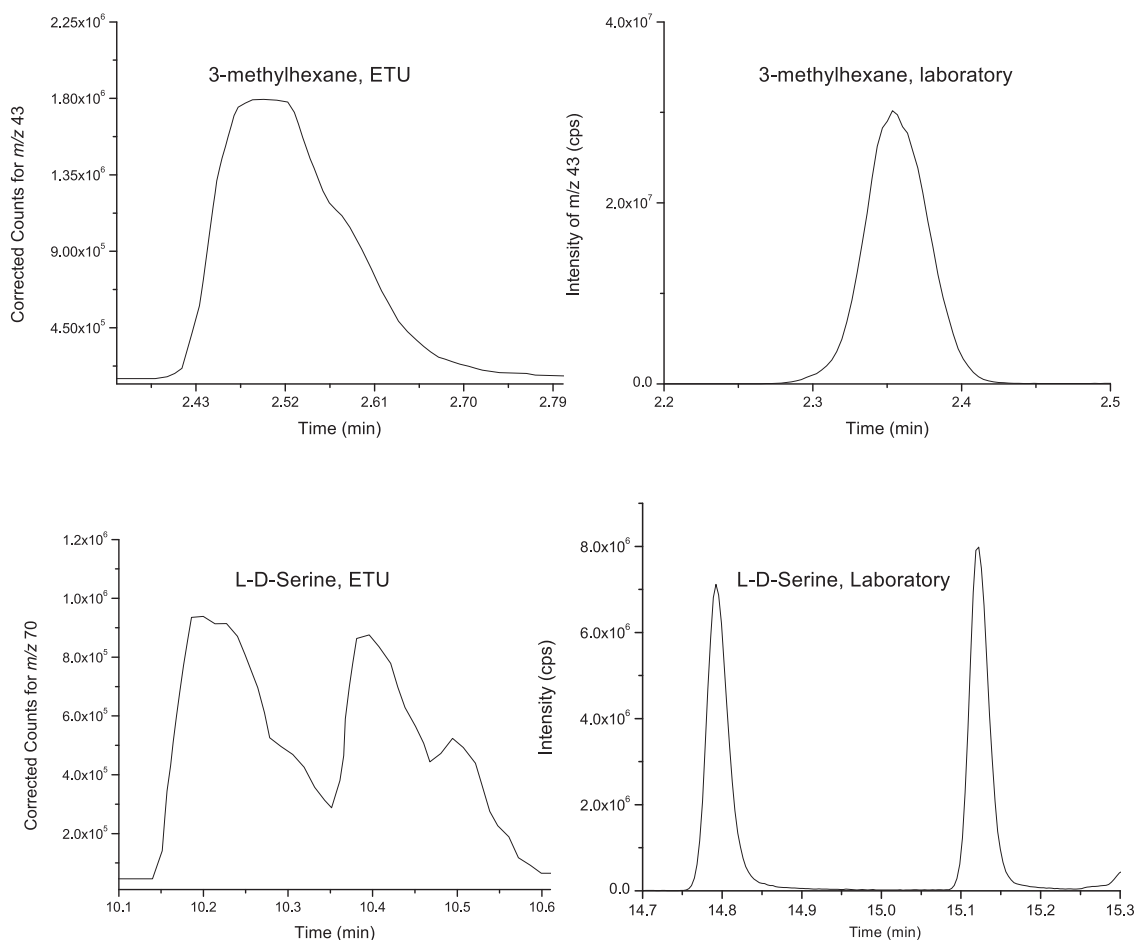
**Fig. 10.** Comparison of MOMA ETU separation of pure chiral 3-methylhexane (top left) and laboratory test (top right). Comparison of MOMA ETU separation of DL-serine (bottom left) and laboratory test (bottom right). The m/z 43 ion is shown for methylhexane and the m/z 70 ion is shown for serine. For the ETU test, the GC column was held isothermally at 35 °C. For the laboratory test, the GC column was held at 35 °C for 7 min and then ramped to 182 °C at a ramp rate of 10°C·min$^{-1}$.

in the form of MTBSTFA and DMF-DMA derivatization enables the detection and identification of additional species of specific astro-biological interest such as amino acids and carboxylic acids, but also complicates gas chromatograms with additional byproduct peaks coming from the derivatization reagent. Therefore, the database built for this study also presents the mass spectra and relative retention times that can be expected from targeted molecules in order to make better identifica-tions of martian organic compounds.

This study shows that the gas chromatographic system of the MOMA experiment is an efficient tool for characterizing complex volatile ma-terials. Its design enables separation and identification of a range of organic species and some inorganic species that could be expected to be present in martian surface and subsurface samples, including a range of alkanes, alcohols, carboxylic acids, as well as amino acids and their en-antiomers. We can expect to detect up to an alkane with 29 carbon atoms using the general purpose (WCOT) columns (MXT 5 and MXT CLP) and up to an alkane with 21 carbon atoms with the chiral column due to its lower maximum temperature of use. Due to the nominal run conditions of the GC system (Table 3), which are constrained by the space experi-ment, we cannot expect to detect all potential compounds of interest. For example, molecules such as mellitic acid, which have up to six derivati-zation sites, are not detectable after either MTBSTFA or DMF-DMA derivatization due to the final molecular weight of the derivatized molecule. The way in which the molecule is altered by derivatization and therefore its characteristics which determine its retention time on the

column (*e.g.*, boiling point, molecular weight) coupled to the character-istics of a given column (*e.g.*, the polarity of the stationary phase, the maximum temperature of use of the column) determine if the molecule is detectable within a nominal MOMA run. The ability of the MOMA gas chromatographic column package to test multiple parameters (*e.g.*, relative abundance of amino acids, enantiomeric excess, patterns in lipid hydrocarbons, chain length distributions as a function of carbon number) enables a confidence value to any potential biosignature detection (Vago et al., 2017).

The MOMA FM recently underwent thermal vacuum testing at TAS-I. Additionally, development of the MOMA testbed is underway at the GSFC and follow-up tests on engineering test units for both the GC, MS, and further coupling campaigns are planned. Although the launch schedule has been recently updated, the plan continues for the ExoMars rover to travel to Mars, with an updated launch date currently projected to be between August and October of 2022. Tests that have been and will be performed on the MOMA FM, testbed, and ETU will allow the refinement of our understanding of the GC-MS instrument capabilities. Further iterations on these types of laboratory studies will enable strict identifications of targeted molecules of astrobiological interest once on Mars.

**Declaration of competing interest**

The authors declare that they have no known competing financial

interests or personal relationships that could have appeared to influence the work reported in this paper.

## CRediT authorship contribution statement

**Melissa Guzman:** Conceptualization, Formal analysis, Investigation, Methodology, Writing - original draft. **Cyril Szopa:** Conceptualization, Formal analysis, Supervision. **Caroline Freissinet:** Conceptualization, Formal analysis, Supervision. **Arnaud Buch:** Conceptualization, Formal analysis, Supervision. **Fabien Stalport:** Conceptualization, Formal analysis, Supervision. **Desmond Kaplan:** Conceptualization, Formal analysis, Supervision. **François Raulin:** Conceptualization, Formal analysis, Supervision.

## Acknowledgements

## References

Altwegg, K., Balsiger, H., Bar-Nun, A., Berthelier, J.-J., Bieler, A., Bochsler, P., Wurz, P., 2016. Prebiotic chemicals—amino acid and phosphorus—in the coma of comet 67P/Churyumov-Gerasimenko. Sci. Adv. 2 (5), e1600285 https://doi.org/10.1126/sciadv.1600285.

Archer, P.D., 2010. The Martian Near Surface Environment: Analysis of Antarctic Soils and Laboratory Experiments on Putative Martian Organics.

Arevalo, R., Brinckerhoff, W., Amerom, F.v., Danell, R., Pinnick, V., Xiang, L., Steininger, H., 2015. Design and demonstration of the mars organic molecule analyzer (MOMA) on the ExoMars 2018 rover. In: Paper Presented at the 2015 IEEE Aerospace Conference, 7-14 March 2015.

Benner, S.A., Devine, K.G., Matveeva, L.N., Powell, D.H., 2000. The missing organic molecules on Mars. Proc. Natl. Acad. Sci. Unit. States Am. 97 (6), 2425–2430. https://doi.org/10.1073/pnas.040539497.

Biemann, K., Oro, J., Toulmin III, P., Orgel, L.E., Nier, A.O., Anderson, D.M., Lafleur, A.L., 1977. The search for organic substances and inorganic volatile compounds in the surface of Mars. J. Geophys. Res. 82 (28), 4641–4658. https://doi.org/10.1029/JS082i028p04641, 1896-1977.

Bowden, S., Parnell, J., 2007. Intracrystalline lipids within sulfates from the haughton impact structure—implications for survival of lipids on mars. Icarus 187, 422–429. https://doi.org/10.1016/j.icarus.2006.10.013.

Brack, A., 2010. Origin of life. In: Cabrol, N., Grin, E. (Eds.), From Habitability to Life on Mars. Elsevier, pp. 13–35.

Brinckerhoff, W.B., Pinnick, V.T., Amerom, F.H. W.v., Danell, R.M., Arevalo, R.D., Atanassova, M.S., Steininger, H., 2013. Mars organic molecule analyzer (MOMA) mass spectrometer for ExoMars 2018 and beyond. In: Paper Presented at the 2013 IEEE Aerospace Conference, 2-9 March 2013.

Buch, A., et al., 2009. Development of a gas chromatography compatible Sample Processing System (SPS) for the in-situ analysis of refractory organic matter in martian soil: preliminary results. Adv. Space Res. 43 (1), 143–151.

Cleaves, H., Chalmers, J., Lazcano, A., Miller, S., Bada, J., 2008. A reassessment of prebiotic organic synthesis in neutral planetary atmospheres. Orig. Life Evol. Biosph. 38, 105–115. https://doi.org/10.1007/s11084-007-9120-3.

Conrad, P.G., Malespin, C.A., Franz, H.B., Pepin, R.O., Trainer, M.G., Schwenzer, S.P., Mahaffy, P.R., 2016. In situ measurement of atmospheric krypton and xenon on Mars with Mars Science Laboratory. Earth Planet Sci. Lett. 454, 1–9. https://doi.org/10.1016/j.epsl.2016.08.028.

Davila, A.F., McKay, C.P., 2014. Chance and necessity in biochemistry: implications for the search for extraterrestrial biomarkers in Earth-like environments. Astrobiology 14 (6), 534–540. https://doi.org/10.1089/ast.2014.1150.

Deamer, D.W., Pashley, R.M., 1989. Amphiphilic components of the murchison carbonaceous chondrite: surface properties and membrane formation. Orig. Life Evol. Biosph. 19 (1), 21–38. https://doi.org/10.1007/bf01808285.

Ehlmann, B.L., et al., 2008. Orbital identification of carbonate-bearing rocks on mars. Science 322 (5909), 1828–1832.

Ehrenfreund, P., Cami, J., 2010. Cosmic carbon chemistry: from the interstellar medium to the early Earth. Cold Spring Harbor Perspect. Biol. 2, a002097. https://doi.org/10.1101/cshperspect.a002097.

Ehrenfreund, P., Charnley, S.B., 2000. Organic molecules in the interstellar medium, comets, and meteorites: a voyage from dark clouds to the early Earth. Annu. Rev. Astron. Astrophys. 38 (1), 427–483. https://doi.org/10.1146/annurev.astro.38.1.427.

Ehrenfreund, P., Glavin, D.P., Botta, O., Cooper, G., Bada, J.L., 2001. Extraterrestrial amino acids in Orgueil and Ivuna: tracing the parent body of CI type carbonaceous

chondrites. Proc. Natl. Acad. Sci. U.S.A. 98 (5), 2138–2141. https://doi.org/10.1073/pnas.051502898.

Eigenbrode, J.L., 2008. Fossil lipids for life-detection: a case study from the early Earth record. Space Sci. Rev. 135 (1), 161–185. https://doi.org/10.1007/s11214-007-9252-9.

Eigenbrode, J.L., Summons, R.E., Steele, A., Freissinet, C., Millan, M., Navarro-González, R., Coll, P., 2018. Organic matter preserved in 3-billion-year-old mudstones at Gale crater, Mars. Science 360 (6393), 1096–1101. https://doi.org/10.1126/science.aas9185.

Elsila, J.E., Glavin, D.P., Dworkin, J.P., 2009. Cometary glycine detected in samples returned by Stardust. Meteoritics Planet Sci. 44 (9), 1323–1330. https://doi.org/10.1111/j.1945-5100.2009.tb01224.x.

Flynn, G.J., 1996. The delivery of organic matter from asteroids and comets to the early surface of Mars. Earth Moon Planets 72 (1), 469–474. https://doi.org/10.1007/bf00117551.

François, P., Szopa, C., Buch, A., Coll, P., McAdam, A.C., Mahaffy, P.R., Cabane, M., 2016. Magnesium sulfate as a key mineral for the detection of organic molecules on Mars using pyrolysis. J. Geophys. Res.: Planets 121 (1), 61–74. https://doi.org/10.1002/2015je004884.

Freissinet, C., Buch, A., Sternberg, R., Szopa, C., Geffroy-Rodier, C., Jelinek, C., Stambouli, M., 2010. Search for evidence of life in space: analysis of enantiomeric organic molecules by N,N-dimethylformamide dimethylacetal derivative dependant Gas Chromatography–Mass Spectrometry. J. Chromatogr. A 1217 (5), 731–740. https://doi.org/10.1016/j.chroma.2009.11.009.

Freissinet, C., Glavin, D.P., Mahaffy, P.R., Miller, K.E., Eigenbrode, J.L., Summons, R.E., Zorzano, M.P., 2015. Organic molecules in the sheepbed mudstone, Gale Crater, mars. J. Geophys. Res. Planets 120 (3), 495–514. https://doi.org/10.1002/2014je004737.

Geffroy-Rodier, C., Grasset, L., Sternberg, R., Buch, A., Amblès, A., 2009. Thermochemolysis in search for organics in extraterrestrial environments. J. Anal. Appl. Pyrol. 85, 454–459. https://doi.org/10.1016/j.jaap.2008.10.005.

Georgiou, D., 2014. Lipids as universal biomarkers of extraterrestrial life. Astrobiology 14 (6), 541–549. https://doi.org/10.1089/ast.2013.1134.

Glavin, D.P., Bada, J.L., Brinton, K.L.F., McDonald, G.D., 1999. Amino acids in the martian meteorite Nakhla. Proc. Natl. Acad. Sci. Unit. States Am. 96 (16), 8835. https://doi.org/10.1073/pnas.96.16.8835.

Glavin, D.P., Elsila, J.E., Burton, A.S., Callahan, M.P., Dworkin, J.P., Hilts, R.W., Herd, C.D.K., 2012. Unusual nonterrestrial l-proteinogenic amino acid excesses in the Tagish Lake meteorite. Meteoritics Planet Sci. 47 (8), 1347–1364. https://doi.org/10.1111/j.1945-5100.2012.01400.x.

Glavin, D.P., Matrajt, G., Bada, J.L., 2004. Re-examination of amino acids in Antarctic micrometeorites. Adv. Space Res. 33 (1), 106–113. https://doi.org/10.1016/j.asr.2003.02.011.

Goesmann, F., Brinckerhoff, W.B., Raulin, F., Goetz, W., Danell, R.M., Getty, S.A., van Amerom, F.H.W., 2017. The mars organic molecule analyzer (MOMA) instrument: characterization of organic material in martian sediments. Astrobiology 17 (6–7), 655–685. https://doi.org/10.1089/ast.2016.1551.

Guzman, M., McKay, C.P., Quinn, R.C., Szopa, C., Davila, A.F., Navarro-González, R., Freissinet, C., 2018. Identification of chlorobenzene in the viking gas chromatograph-mass spectrometer data sets: reanalysis of viking mission data consistent with aromatic organic compounds on mars. J. Geophys. Res.: Planets 123 (7), 1674–1683. https://doi.org/10.1029/2018je005544.

He, Y., Buch, A., Morisson, M., Szopa, C., Freissinet, C., Williams, A., Johnson, S.S., 2019. Application of TMAH thermochemolysis to the detection of nucleobases: application to the MOMA and SAM space experiment. Talanta 204, 802–811. https://doi.org/10.1016/j.talanta.2019.06.076.

Hecht, M.H., Kounaves, S.P., Quinn, R.C., West, S.J., Young, S.M.M., Ming, D.W., Smith, P.H., 2009. Detection of perchlorate and the soluble chemistry of martian soil at the Phoenix lander site. Science 325 (5936), 64–67. https://doi.org/10.1126/science.1172466.

Hennet, R.J.-C., Holm, N.G., Engel, M.H., 1992. Abiotic synthesis of amino acids under hydrothermal conditions and the origin of life: a perpetual phenomenon? Naturwissenschaften 79 (8), 361–365. https://doi.org/10.1007/bf01140180.

Kaplan, Desmond, Guzman, Melissa, Stalport, Fabien, Grande, Noel, Szopa, Cyril, Freissinet, Caroline, Buch, Arnaud, Grubisic, Andrej, Danell, Ryan M., Van Amerom, Friso, Li, Xiang, Getty, Stephanie A., Brinckerhoff, William B., Mahaffy, Paul R., 2019. Demonstration and verification of the pyrolysis and derivatization GCMS capabilities of the mars organic molecule analyzer (MOMA) mass spectrometer. In: Paper Presented at the ASMS Conference on Mass Spectrometry and Allied Topics, Atlanta.

Kennedy, M.J., Pevear, D.R., Hill, R.J., 2002. Mineral surface control of organic carbon in Black Shale. Science 295 (5555), 657–660. https://doi.org/10.1126/science.1066611.

Knapp, D.R., 1979. Handbook of Analytical Derivatization Reactions. Wiley-Interscience, New York.

Kobayashi, K., Kasamatsu, T., Kaneko, T., Koike, J., Oshima, T., Saito, T., Yanagawa, H., 1995. Formation of amino acid precursors in cometary ice environments by cosmic radiation. Adv. Space Res. 16 (2), 21–26. https://doi.org/10.1016/0273-1177(95)00188-K.

Lasne, J., Noblet, A., Szopa, C., Navarro-González, R., Cabane, M., Poch, O., Coll, P., 2016. Oxidants at the surface of mars: a review in light of recent exploration results. Astrobiology 16 (12), 977–996. https://doi.org/10.1089/ast.2016.1502.

Leshin, L.A., Mahaffy, P.R., Webster, C.R., Cabane, M., Coll, P., Conrad, P.G., Grotzinger, J.P., 2013. Volatile, isotope, and organic analysis of martian fines with the mars curiosity rover. Science 341 (6153), 1238937. https://doi.org/10.1126/science.1238937.

Li, X., Danell, R., Brinckerhoff, W., Pinnick, V., Amerom, F., Arevalo Jr., R., Goesmann, F., 2015. Detection of trace organics in mars analog samples containing perchlorate by laser desorption/ionization mass spectrometry. Astrobiology 15. https://doi.org/10.1089/ast.2014.1203.

Mahaffy, P.R., Webster, C.R., Cabane, M., Conrad, P.G., Coll, P., Atreya, S.K., Mumm, E., 2012. The sample analysis at mars investigation and instrument suite. Space Sci. Rev. 170 (1), 401–478. https://doi.org/10.1007/s11214-012-9879-z.

Marshall, W.L., 1994. Hydrothermal synthesis of amino acids. Geochem. Cosmochim. Acta 58 (9), 2099–2106. https://doi.org/10.1016/0016-7037(94)90288-7.

Maurette, M., 1998. Carbonaceous micrometeorites and the origin of life. Orig. Life Evol. Biosph. 28 (4), 385–412. https://doi.org/10.1023/a:1006589819844.

Mawhinney, T.P., Madson, M.A., 1982. N-Methyl-N-(tert-butyldimethylsilyl) trifluoroacetamide and related N-tert-butyldimethylsilyl amides as protective silyl donors. J. Org. Chem. 47 (17), 3336–3339. https://doi.org/10.1021/jo00138a032.

McKay, D.S., et al., 1996. Search for past life on mars: possible relic biogenic activity in martian meteorite ALH84001. Science 273 (5277), 924–930.

Meierhenrich, U., Cason, J., Szopa, C., Sternberg, R., Raulin, F., Thiemann, W., Goesmann, F., 2013. Evaluating the robustness of the enantioselective stationary phases on the Rosetta mission against space vacuum vaporization. Adv. Space Res. 52, 2080–2084. https://doi.org/10.1016/j.asr.2013.09.018.

Meierhenrich, U.J., Thiemann, W.H.-P., Goesmann, F., Roll, R., Rosenbauer, H., 2001. Enantiomer separation of hydrocarbons in preparation for ROSETTA's "chirality-experiment". Chirality 13 (8), 454–457. https://doi.org/10.1002/chir.1061.

Millan, M., Szopa, C., Buch, A., Coll, P., Glavin, D., Freissinet, C., Mahaffy, P., 2016. In situ analysis of martian regolith with the SAM experiment during the first mars year of the MSL mission: identification of organic molecules by gas chromatography from laboratory measurements. Planet. Space Sci. 129 https://doi.org/10.1016/j.pss.2016.06.007.

Miller, K.E., Eigenbrode, J.L., Freissinet, C., Glavin, D.P., Kotrc, B., Francois, P., Summons, R.E., 2016. Potential precursor compounds for chlorohydrocarbons detected in Gale Crater, Mars, by the SAM instrument suite on the Curiosity Rover. J. Geophys. Res.: Planets 121 (3), 296–308. https://doi.org/10.1002/2015je004939.

Morris, R.V., et al., 2010. Identification of carbonate-rich outcrops on mars by the spirit rover. Science 329 (5990), 421–424.

Myrgorodska, I., Javelle, T., Meinert, C., Meierhenrich, U.J., 2016. Enantioselective gas chromatography in search of the origin of biomolecular asymmetry in outer space. Isr. J. Chem. 56 (11–12), 1016–1026. https://doi.org/10.1002/ijch.201600067.

Naraoka, H., Shimoyama, A., Harada, K., 1999. Molecular distribution of monocarboxylic acids in Asuka carbonaceous chondrites from Antarctica. Orig. Life Evol. Biosph. 29 (2), 187–201. https://doi.org/10.1023/a:1006547127028.

Navarro-González, R., Vargas, E., de la Rosa, J., Raga, A.C., McKay, C.P., 2010. Reanalysis of the Viking results suggests perchlorate and organics at midlatitudes on Mars. J. Geophys. Res.: Planets 115 (E12). https://doi.org/10.1029/2010je003599.

Oró, J., Holzer, G., 1979. The photolytic degradation and oxidation of organic compounds under simulated Martian conditions. J. Mol. Evol. 14 (1), 153–160. https://doi.org/10.1007/bf01732374.

Pavlov, A.A., Vasilyev, G., Ostryakov, V.M., Pavlov, A.K., Mahaffy, P., 2012. Degradation of the organic molecules in the shallow subsurface of Mars due to irradiation by cosmic rays. Geophys. Res. Lett. 39 (13) https://doi.org/10.1029/2012GL052166.

Peltzer, E.T., Bada, J.L., Schlesinger, G., Miller, S.L., 1984. The chemical conditions on the parent body of the murchison meteorite: some conclusions based on amino, hydroxy and dicarboxylic acids. Adv. Space Res. 4 (12), 69–74. https://doi.org/10.1016/0273-1177(84)90546-5.

Pizzarello, S., Cooper, G., Flynn, G., 2006. The Nature and Distribution of the Organic Material in Carbonaceous Chondrites and Interplanetary Dust Particles. Meteorites and the Early Solar System II.

Pizzarello, S., Garvie, L.A.J., 2014. Sutter's Mill dicarboxylic acids as possible tracers of parent-body alteration processes. Meteoritics Planet Sci. 49 (11), 2087–2094. https://doi.org/10.1111/maps.12264.

Poch, O., Kaci, S., Stalport, F., Szopa, C., Coll, P., 2014. Laboratory insights into the chemical and kinetic evolution of several organic molecules under simulated Mars

surface UV radiation conditions. Icarus 242, 50–63. https://doi.org/10.1016/j.icarus.2014.07.014.

Poulet, F., Carter, J., Riu, L., Martinez, A., 2019. Modal Mineralogy of Phyllosilicate- and Carbonate-Bearing Terrains from Spectral Modeling. Application to Mars2020 and ExoMars Landing Sites. LPI Contributions, 2089.

Quantin, C., Carter, J., Thollot, P., Broyer, J., Lozach, L., Davis, J., Ody, A., 2016. Oxia Planum, the landing site for ExoMars 2018. In: Paper Presented at the 47th Lunar and Planetary Science Conference, Houston.

Rampe, E.B., Lapotre, M.G.A., Bristow, T.F., Arvidson, R.E., Morris, R.V., Achilles, C.N., Treiman, A.H., 2018. Sand mineralogy within the Bagnold Dunes, Gale Crater, as observed in situ and from orbit. Geophys. Res. Lett. 45 (18), 9488–9497. https://doi.org/10.1029/2018gl079073.

Sephton, M.A., 2005. Organic matter in carbonaceous meteorites: past, present and future research. Phil. Trans. Math. Phys. Eng. Sci. 363 (1837), 2729–2742. https://doi.org/10.1098/rsta.2005.1670.

Sephton, M.A., 2012. Pyrolysis and mass spectrometry studies of meteoritic organic matter. Mass Spectrom. Rev. 31 (5), 560–569. https://doi.org/10.1002/mas.20354.

Sephton, M.A., Botta, O., 2008. Extraterrestrial organic matter and the detection of life. Space Sci. Rev. 135 (1), 25–35. https://doi.org/10.1007/s11214-007-9171-9.

Shimoyama, A., Shigematsu, R., 1994. Dicarboxylic acids in the murchison and Yamato-791198 carbonaceous chondrites. Chem. Lett. 23 (3), 523–526. https://doi.org/10.1246/cl.1994.523.

Siljeström, S., et al., 2014. Comparison of prototype and laboratory experiments on MOMA GCMS: results from the AMASE11 campaign. Astrobiology 14 (9).

Stalport, F., Coll, P., Szopa, C., Cottin, H., Raulin, F., 2009. Investigating the photostability of carboxylic acids exposed to mars surface ultraviolet radiation conditions. Astrobiology 9, 543–549. https://doi.org/10.1089/ast.2008.0300.

Stalport, F., Rouquette, L., Poch, O., Dequaire, T., Chaouche-Mechidal, N., Payart, S., Cottin, H., 2019. The photochemistry on space station (PSS) experiment: organic matter under mars-like surface UV radiation conditions in low Earth orbit. Astrobiology 19 (8), 1037–1052. https://doi.org/10.1089/ast.2018.2001.

Stoker, C.R., Bullock, M.A., 1997. Organic degradation under simulated Martian conditions. J. Geophys. Res.: Planets 102 (E5), 10881–10888. https://doi.org/10.1029/97je00667.

Summons, R., Albrecht, P., McDonald, G., Moldowan, J., 2008. Molecular biosignatures. Space Sci. Rev. 135, 133–159. https://doi.org/10.1007/s11214-007-9256-5.

Sutter, B., McAdam, A.C., Mahaffy, P.R., Ming, D.W., Edgett, K.S., Rampe, E.B., Yen, A.S., 2017. Evolved gas analyses of sedimentary rocks and eolian sediment in Gale Crater, Mars: results of the Curiosity rover's sample analysis at Mars instrument from Yellowknife Bay to the Namib Dune. J. Geophys. Res.: Planets 122 (12), 2574–2609. https://doi.org/10.1002/2016je005225.

Szopa, C., et al., 2002. Gas chromatography for in situ analysis of a cometary nucleus III. Multi-capillary column system for the cometary sampling and composition experiment of the Rosetta lander probe. J. Chromatogr. A 953 (1–2), 165–173.

Szopa, C., et al., 2004. Dual column capillary gas chromatographic system for the in situ analysis of volatile organic compounds on a cometary nucleus. J. Sep. Sci. 27 (7–8), 495–503.

Szopa, C., Freissinet, C., Glavin, D.P., Millan, M., Buch, A., Franz, H.B., Sumner, D., Mahaffy, P.R., Sutter, B., Eigenbrode, J.L., Williams, R.H., Navarro-González, R., Guzman, M., Malespin, C., Teinturier, S., Mahaffy, P.R., Cabane, M., 2020. First detections of dichlorobenzene isomers and trichloromethylpropane from organic matter indigenous to mars mudstone in Gale Crater, mars: results from the sample analysis at mars instrument onboard the curiosity rover. Astrobiology 20 (2), 292–306.

ten Kate, I.L., Garry, J.R.C., Peeters, Z., Foing, B., Ehrenfreund, P., 2006. The effects of Martian near surface conditions on the photochemistry of amino acids. Planet. Space Sci. 54 (3), 296–302. https://doi.org/10.1016/j.pss.2005.12.002.

Vago, J., Team, t., incuding, Duxbury, N., 2017. Habitability on early mars and the search for biosignatures with the ExoMars rover. Astrobiology 17, 471–510.